ABSTRACT

Title of Document: **ON DETERMINING SPONTANEOUS IGNITION IN POROUS MATERIALS**

Stephen Michael Tamburello, Master of Science in Fire Protection Engineering, 2011

Directed By: Professor, Dr. James G. Quintiere, Ph.D., Department of Fire Protection Engineering

A guide is developed that lays out the process of analyzing spontaneous ignition likelihood. The Frank-Kamenetskii (F-K) theory forms the basis of the approach. The Damkohler number, defined as the dimensionless heat generation parameter for a self-heating body, is described in terms of two key material constants and these materials are related to real incident spontaneous ignition scenarios. The Damkohler number is compared to the critical Damkohler number, value of heat generation at the onset of runaway condition, to determine if spontaneous ignition is likely. Corrections to the critical Damkohler number are described for cases of finite Biot number, low activation energy, and reactant consumption. Heat transfer analysis is needed in terms of a Biot number, and its calculation is described. A specific measurement of the heat transfer in an oven is described. Application of the spontaneous ignition hazard analysis for a real case is presented.

ON DETERMINING SPONTANEOUS IGNITION IN POROUS MATERIALS

By

Stephen Michael Tamburello

Thesis submitted to the Faculty of the Graduate School of the
University of Maryland, College Park, in partial fulfillment
of the requirements for the degree of
Master of Science
2011

Advisory Committee:
Professor James G. Quintiere, Ph.D., Chair
Assistant Professor Stanislav I. Stoliarov, Ph.D.
Associate Professor Peter B. Sunderland, Ph.D.

Preface

This project was support by the National Institute of Justice to further the knowledge and analysis of spontaneous ignition for fire investigations. This thesis was intended to help fire investigators diagnose the occurrence of spontaneous ignition for self-heating materials. The focus of this study was to present a mathematical model that can be a tool for forensic fire labs, and increase the accuracy of results by examining heat transfer characteristics for testing materials.

Acknowledgements

This study was made possible by the financial support of the National Institute of Justice to improve forensic analysis of spontaneous ignition. We hope this work will give the investigator a greater understanding of spontaneous ignition that will enable its recognition, and establish testing and analysis techniques to support its likelihood. A special thanks to Thomas E. Minnich from the National Center for Forensic Science (NCFS) at The University of Central Florida for his expertise and collaboration between NCFS and The University of Maryland's Department of Fire Protection Engineering.

A special thanks to my advisor, Dr. James Quintiere, for his continuous service as a leader and mentor ensuring the accomplishment of my goal.

Table of Contents

List of Tables

List of Figures

Nomenclature

A = pre-exponential factor [s^{-1}]

$A_{oven} = 2WH + 2WD + 2HD$

c = specific heat of the basket [461 *J/kg-K*]

E = activation energy [*kJ/mol*]

F_{12} = view factor = 1 for parallel plates

g = gravity [9.81 m/s^2]

h = basket heat transfer coefficient

H = basket height [m]

r = half-width of object

R = universal gas constant [8.314x10^{-3} *kJ/mol-K*]

m = mass of the basket [kg]

Q = heat of reaction [*kJ/kg*]

S = surface area of basket = $5 * H^2$

T_A = ambient temperature [K]

T_i = initial material temperature [K]

T_P = hot plate temperature [K]

T_R = reference temperature [K]

T_S = basket surface temperature [K]

Greek

α = Biot number = $\frac{hr}{\lambda}$

$\beta = \frac{1}{T_{film}}$ = volumetric thermal expansion [K^{-1}]

ϵ_s = emissivity of the basket

ϵ_o = emissivity of the oven

κ_f = kinematic viscosity of air at T_{film} [m^2/s]

λ_S = thermal conductivity of the material [*W/m-K*]

λ_f = thermal conductivity of air

ν_f = kinematic viscosity of air at T_{film} [m^2/s]

u_∞ = measured air velocity in convection oven [1.6 m/s]

ρ = material density [kg/m^3]

σ = Stefan-Boltzmann constant [5.67*10^{-8} W/m^2-K]

Chapter 1: Introduction to Spontaneous Ignition

Self-heating refers to the exothermic reaction of an unstable material leading to an internal temperature rise due to limited thermal conductivity within a material. Any substance that possesses exothermiscity, by itself or in the presence of air, is prone to an unstable condition in which its internal temperature can increase significantly due to the heat released from a chemical reaction. This reaction can be a decomposition of the substance, or oxidation. An example of an exothermic substance is ammonium perchlorate ($NH_4\ ClO_4$) or wood fiberboard. Gaseous products from the reaction can be trapped causing large pressure increase or fissures in the material. With a sufficient internal temperature increase, an accelerating reaction front can propagate through the material. The internal temperature can increase high enough, with sufficient available oxygen, so that smoldering conditions may occur. Eventually, the smoldering can transition to flaming. The initiation of smoldering or flaming conditions here is referred to as spontaneous ignition or thermal explosion.

ASTM E-659 (ASTM Standard E659-78, 2005) is a standard test to analyze the spontaneous ignition of liquid heated to vapor in air. It does this by measuring the minimum furnace temperature to cause a flame in a 500 ml spherical flask containing several drops of the evaporated liquid. Spontaneous ignition for gaseous fuels in air occurs at the onset of a flame and the minimum temperature to cause ignition is called the auto-ignition temperature. While auto-ignition temperatures are typically listed for liquids and gases, these values will vary depending on the size of the flask, the conditions of heating, and the configuration of the flammable mixture. For example, the same fuel tested in ASTM E-659 and tested on a hot surface, the test on a hot surface will require a

much higher temperature for spontaneous ignition. NFPA claims an increase of 200 ^{o}C will be needed for ignition, but the temperature increase required can be more. The hot surface case will require a higher auto-ignition temperature due to the heat source only being adjacent to the bottom of the flask.

This thesis focuses on spontaneous ignition of porous oxidizing or exothermically decomposing solids. To determine if spontaneous ignition may occur, the rate at which heat is generated from the exothermic reaction can be compared to the rate of heat released from the material to the surroundings. When the rate of heat generated is less than the rate of heat escaped, the material will remain steady until all reactive material is depleted. In contrast, if the material is generating heat at a higher rate than can be released, the temperature within the material will rapidly increase, known as thermal runaway.

In determining the behavior of spontaneous ignition for porous solids, a combination of parameters is examined. The main parameter is the critical ambient temperature (CAT), which is the surrounding air temperature that creates the onset of ignition. This value may be obtained experimentally with a standard oven test, where a stainless steel wire-mesh basket is filled with reactive material and heated at a constant temperature in a convection oven (Bowes, 1984). The test is repeated at different temperatures until the minimum temperature to cause ignition is obtained. The CAT of a material can vary greatly with material volume, shape, and heating configuration; therefore, a mathematical model is needed to correlate results over a range of material sizes. Frank-Kamenetskii (1939) developed the first mathematical model allowing the

means of determining conditions needed for spontaneous ignition, as well as a correlation for scaling critical temperatures with varying material sizes.

The Frank-Kamenetskii model (F-K) uses a dimensionless heat generation parameter for a pile of material called the Damkohler number (δ) and compares it to the critical Damkohler number (δ_c), which is the critical value of heat generation to cause ignition. If $\delta \geq \delta_c$, ignition will occur. The use of the Frank-Kamenetskii model with oven tests will be described for different fire scenarios and material shapes. Material properties that do not vary with material configuration, *P* and *M*, and the method of determining these properties will be described. *P* is the ratio of the activation energy (*E*) for the material to the universal gas constant (*R*), and *M* is a combination of variables from the Damkohler number that do not vary with body size or temperature under F-K theory assumptions.

Note that the Frank-Kamenetskii model is simplified and ignores many factors such as the diffusion of oxygen, moisture, non-conduction heating within the substance, mixtures with competing reactions, and transient effects. Since many factors are neglected in this theory, its results in practice should only be used as a guide to interpreting the spontaneous ignition. The fire scenarios for a cold material in a hot environment, material on a hot plate, and hot material in a cold environment described later are ideal, and their application to real event scenarios are not likely to be perfect. This factor, as well as effects ignored in the theory, is responsible for the cautionary considerations in making predictions; however, it is the only tool that can be applied without the consideration of complex factors that may not stand the test of accuracy in their modeling. Still, this approach will give reasonable results provided the input data

do not vary with scale. One important deficiency is that data obtained at temperatures above the melting point will not conform to exposure conditions below the melting point. The material would lose its integrity by melting at the high temperature, while the outside of the material will retain solid integrity at the low temperature.

In practice, the F-K method can be used to examine a real fire scenario in the following manner:

1. Find δ_c for the given scenario. This parameter depends on the shape of the material body and the heating configuration being analyzed. Details on finding δ_c are given in Chapter 3 for the heating configurations of a cold body in a hot environment (Section 3.3), material layer on a hot surface (Section 3.4), and a hot body in a cold environment (Section 3.5). This parameter may need to be adjusted if assumptions in Section 3.2.1 are not met. Adjustment calculations are given within Sections 3.3, 3.4, and 3.5.
2. Use a testing method, such as the oven basket method, to find the CAT for multiple size baskets. The CAT values will change if the Biot number for the basket and the surroundings is not large. The Biot number is large when the basket surface temperature remains approximately the same as the oven temperature, which is typically present in an oven basket test through high fan speed. In the event that this value is not large, a correction can be made to δ_c by following the heat transfer method provided in Chapter 5 and using the Biot correction in Section 3.3.2.
3. Find the material constants, *P* and *M*, using the data produced by the standard oven basket test.

Section 4.2 gives a general description for finding these properties. Section 4.5 is a compilation of P and M values from various sources.

4. For the calculated P and M constants and the given half-width (r) from the real fire scenario, the minimum ambient temperature to cause ignition may be found, as seen in Section 4.6. If the surrounding air temperature is higher than the calculated critical temperature, ignition is likely to occur. The calculated critical temperature is only a rough estimate, so caution should be taken when analyzing the likelihood of spontaneous ignition.

The purpose of this study is to provide fire investigators with:

1. A guide of determining spontaneous ignition hazard for porous solids in three fire scenarios: cold material in a hot environment, material layer on a hot surface, and hot material in a cold environment.
2. A method of experimentally finding material constants, P and M, for self-heating materials.
3. A database of listed P and M values.
4. An experimental procedure for finding the heat transfer coefficient between material and its surroundings in oven basket tests.

Chapter 2: Background

Many common materials such as fertilizers, animal feedstuff, grass, wood, and grains are known to generate heat during decomposition. In combination with the magnitude of the volume of material and the exposure temperature, these materials can undergo spontaneous ignition. Many self-heating fire cases result in large fires that make investigations difficult due to the destruction of evidence; however, the trend points to the phenomenon as the cause (Gray, 2002). Spontaneous ignition is often difficult to investigate and even overlooked. The hazard of spontaneous ignition has led to numerous fatalities and costly property damage.

February 23, 1991 a high-rise office building fire occurred at One Meridian Plaza in Philadelphia, Pennsylvania. The fire was caused by the spontaneous ignition of linseed oil on cotton rags. The innocent resulted in the fatalities of three Philadelphia firefighters and an estimated $100 million in direct property loss. The litigation resulted in approximately $4 billion in civil damage claims (Routley, Jennings, & Chubb, 1991).

Mitchell (1951), discussed a fire that occurred in the summer of 1950 that caused $2,609,000 in damages. According to Mitchell's article, nine freight cars of wood fiberboard were being delivered from a manufacturer in the South to an Army Warehouse in upstate New York. Seven days into shipment and only a few miles from its destination, one of the freight cars was discovered in flames. The car was left in the railyard and the remaining eight continued to the Army Warehouse where the fiberboard was unloaded into one pile. Two days after being unloaded, the fiberboard pile ignited destroying the warehouse and its contents. Tests of wood fiberboard specimens later determined that the fire causes were due to spontaneous ignition (Mitchell, 1951).

Another common material that has caused countless accidental fires due to spontaneous combustion is calcium hypochlorite. In July of 1999, a containership ship, *CMA Djakarta*, carrying a dry form of calcium hypochlorite set fire while sailing south of Crete. The 21-member crew was required to abandon the 1998-built ship as the fire started among the containers on deck. Efforts to extinguish the flames were unsuccessful as the flame continuously re-ignited due to the high ambient temperatures off the coast of Egypt (Darling, 1999).

In December of 1998, another anhydrous form of calcium hypochlorite was reported to ignite the cargo ship *CMA Aconcagua* while sailing off the Ecuadorian coast. The crew safely evacuated, though damages to the ship and cargo loss were estimated between $15-18 million. As opposed to the incident on the *Djakarta*, the *Aconcagua* held the calcium hypochlorite below deck where temperatures may rise above ambient (Darling, 1999).

One month prior to the *Aconcagua* incident, an explosion occurred on the *DG Harmony* off the coast of Brazil. According to the United States Court of Appeals for the Second Circuit ruling for the *Harmony* explosion, the ship was carrying approximately 160,000 kilograms of calcium hypochlorite below deck. On November 9th, an explosion occurred in the area where the calcium hypochlorite was being held. The crew attempted to fight the fire for 12 hours before abandoning the vessel and the ship continued to burn for 3 weeks (DG Harmony v. PPG Industries Inc., 2008). Though there were no casualties, the estimated damage was $16 million (Darling, 1999).

Another explosion on the vessel *Contship France* occurred in October of 1997. The ship had 512 drums of calcium hypochlorite (Contship Containerline Ltd. v. PPG

Industries Inc., 2006) aboard while docked in Papeete Harbor, Tahiti. The explosion was originally thought to have been caused from a cargo of aerosol spray cans, until further investigation led to the self-heating of calcium hypochlorite contained in the area of the explosion (Darling, 1999). The court ruling acknowledged that temperatures in the cargo area were high enough for the calcium hypochlorite to spontaneously ignite resulting in the cause of the explosion.

The previous accounts of cargo vessel fires were the result of dry calcium hypochlorite. The chemical is also available in a more reactive hydrated form, which must be kept on deck during marine vessel transport. In 1993, the Russian cargo ship *Kapitan Sakharov* set fire due to the self-heating of a hydrated calcium hypochlorite. Though the chemical was transported on deck, it is believed that radiation from the sun provided sufficient heat for spontaneous ignition to occur. In addition to the vast financial damage, two fatalities occurred due to the fire (Darling, 1999).

Power companies and coalmines are familiar with the hazards of coal dust. Several fires have occurred in the past decade due to coal dust spontaneously combusting, including one in Gillette, Wyoming. In June of 2004 at the Buckskin mine in a fire occurred at a storage warehouse causing $200,000 in damages. According to the fire investigator, the cause of the fire was most likely the spontaneous ignition of coal dust that collected in the warehouse (The Gillette News, 2004).

The occurrences of extensive damage from spontaneous ignition mentioned are only a few examples of countless events throughout history. The phenomena of self-heating can cause millions of dollars in asset loss and hundreds of fatalities. In the investigation of similar occurrences, spontaneous ignition is often a neglected cause of

fire or misdiagnosed. The scope of this project will give an investigator a greater understanding of spontaneous ignition that will enable its recognition, and establish testing and analysis techniques to support its likelihood.

Chapter 3: Self-Heating

3.1 General Description of Spontaneous Ignition

The occurrence of spontaneous ignition in porous solids is simplified into two attributes of a material body: the internal heat generation rate, and the heat release rate to surroundings. The rate of heat that escapes from a reactive pile to the environment is dependent on the size, shape, and thermal conductivity of the material. A large pile size as well as a low conductivity will restrict heat release, therefore, increasing the probability of spontaneous ignition. The heat generation within the pile is related to the reactivity of the material and the temperature inside the body. Most exothermic oxidation reactions become more reactive with higher temperatures, so heat generation increases with rising body temperatures. In general, the pile is stable as long as the rate of heat generated is less than the rate at which heat can be released from the material. If the pile reaches conditions in which the rate of heat generation is faster than the release rate, the center temperature of the material will increase. In most cases the increase of center temperature will cause the central heat generation to increase, leading to thermal runaway and ultimately ignition. With sufficient available oxygen to the center of the material, flaming conditions may occur. The oxygen needed for ignition can be supplied from diffusion or buoyant flow.

A scientific model for determining the likelihood of spontaneous ignition for a known pile size and ambient conditions has been developed by Frank-Kamenetskii (Frank-Kamenetskii, 1939) and examined by Bowes (Bowes, 1984). Frank-

Kamenetskii's model uses a dimensionless heat generation parameter, called the Damkohler number (δ),

$$\delta = \frac{E/R}{T_R}\frac{\rho A Q}{\lambda}\frac{r^2}{T_R}\exp\left(\frac{-E/R}{T_R}\right) \tag{3.1}$$

and compares it to the Critical Damkohler number, δ_c. When $\delta > \delta_c$, spontaneous ignition occurs. The Critical Damkohler number varies with the geometric condition, and the computations are explained for material in the following three common scenarios: (1) pile in a hot environment, (2) material on a hot surface, and (3) hot material in cool environment.

3.2 Self-Heating Theory

3.2.1 Assumptions to the Theory

The Frank-Kamenetskii theory derivation is valid under certain assumptions. These assumptions are developed by Frank-Kamentskii (Frank-Kamenetskii, 1939) and listed by Paula F. Beever (Beever P. F., 1988).

1.) A single zeroth order exothermic reaction generates heat as a function of temperature only. Also, there is no depletion or consumption of reactants due to the heat generation reaction.

2.) The activation energy is high enough for the condition

$$\varepsilon = \frac{RT_A}{E} << 1 \tag{3.2}$$

to hold true, where T_A is the ambient temperature.

3.) Conduction accounts for the heat transfer within the body.

4.) Convective and radiative heat transfer between the body surface and surroundings is enough so that the body surface temperature remains approximately equal to the surrounding air temperature. High heat transfer between the body and environment implies the Biot Number, α, approaches infinity such that:

$$\alpha = \frac{hr}{\lambda} \rightarrow \infty \tag{3.3}$$

If the Biot number is finite (not large), adjustments to δ_c are needed (Section 3.3.2 of this thesis)

It is important that the assumptions listed are met to ensure accuracy of the spontaneous ignition criteria. A high heat transfer between the reactive body and surroundings is achieved with a high oven fan speed. The high convection from an oven fan is easily applied in oven tests; however, fire incidents will often have low air velocities at the reactive material. Low heat transfer between the body and surroundings, depletion of the reactive material, and low activation energy cause inaccuracy in the Damkohler number, in which it is necessary to use corrections.

3.2.2 Introduction to Self-Heating Theory

The basis of the theory was developed by Frank-Kamenetskii and evaluated by Bowes (1984). The results and notation from Bowes will be used. The basic energy conduction equation with a uniform energy generation rate due to an exothermic chemical reaction is given as

$$\rho c \frac{\partial T}{\partial t} = \nabla \cdot \lambda \nabla T + \dot{q}''' \tag{3.4}$$

where, the heat generation term with no depletion is assumed to follow the Arrhenius Equation, given by:

$$\dot{q}''' = Q\rho Ae^{-E/RT} \tag{3.5}$$

The pre-exponential factor, A, can depend on temperature, and the concentration of the reactants. Hence when the reactants are consumed from the heat generation reaction, A goes to zero as there is no energy generation. A plot of $\dot{q}'''$ with temperature is sketched in Figure 3.1 for A constant (no depletion).

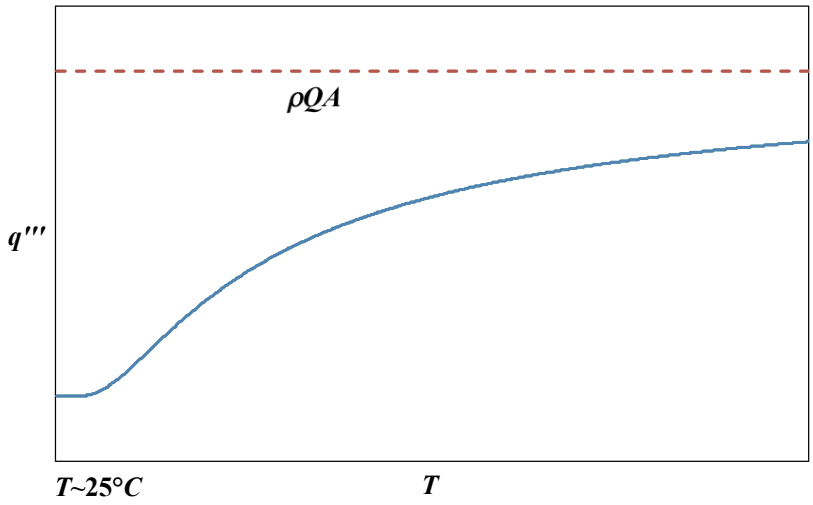

Figure 3.1: Internal heat generation with no depletion as a function of temperature.

The rate of heat generation reaches a maximum of ρQA as T→∞, and the values of $\dot{q}'''$ can range as low as 10^{-15} W/cm^3 at normal ambient temperature to 10^{10} W/cm^3 at flame temperatures. If A drops as reactants are depleted, the curve in Figure 3.1 collapses to the horizontal axis. In Equation 3.4, as long as the generation term is greater than the conduction term, the temperature will increase in the material. Even if a steady condition

is reached the material will be higher than its surroundings, as the generation must equal the conduction loss.

For a pile in uniform surroundings, the center temperature would be highest. Bowes considers such a case, and sketches the center temperature (T_o) relative to the ambient temperature (T_A). The lower curve (0-I) in Figure 3.2 represents steady conditions for this reaction.

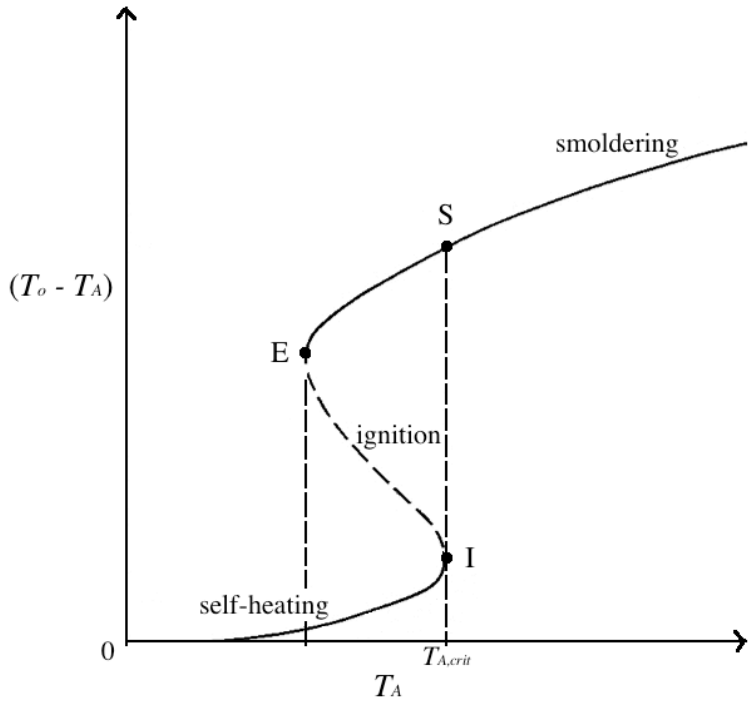

Figure 3.2: Material center and ambient temperature differences as a function of the ambient temperature (Bowes, 1984)

The upper curve from E represents steady conditions once ignition occurs to a smoldering reaction. The level of the E curve will increase as the diffusion of oxygen dies. The ambient temperature at I is the temperature needed for spontaneous ignition to smoldering. The new steady state to S involves a jump in T_o. The E point is the extinction of the smoldering reaction, and the curve I-E is unstable. In reality, the

depletion of reactants would make the process unsteady. A sketch of this is shown below where two different outcomes occur for T_A less than and greater than its critical value at I, $T_{A,crit}$.

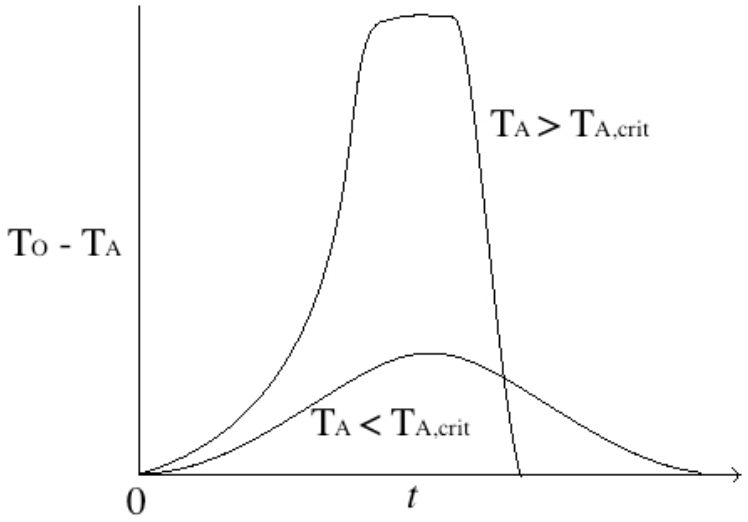

Figure 3.3: Critical ($T_A > T_{A,crit}$) and subcritical ($T_A < T_{A,crit}$) heating curves

There is a more significant temperature rise above the critical condition for ignition. Alternatively, the size of the pile at a fixed T_A could have a critical condition for this large temperature rise or "ignition". Here the ignition outcome is depicted as steady smoldering, but flow changes in the pile at this jump in temperature could lead to flaming.

3.2.3 Steady Analysis

With no reaction depletion, two outcomes are possible: (1) a steady solution exists where the center temperature becomes constant ($T_0 > T_A$), (2) no steady solution exists and

the internal temperature will lead to thermal runaway. In the approximate theory of F-K to follow, the non-steady case will cause the internal temperature to become infinite. In real cases, ignition to smoldering or flaming prevents an infinite rise. Hence, the approach is to examine problem scenarios governed by Equations 3.4 and 3.5 for which the point of no steady solution is found. This is the "critical condition" that makes the boundary between a stable steady solution and ignition or thermal runaway. In this way the conditions for spontaneous ignition are found.

Analyzing the steady state condition of the energy balance, the left-hand side remains constant and, by definition, is zero. This reduces Equation 3.4:

$$-\nabla \cdot \lambda \nabla T = \dot{q}'' \tag{3.6}$$

Next, Equations 3.5 and 3.6 can be non-dimensionalized with the identity,

$$-\frac{E}{RT} \equiv -\frac{E}{RT_A} + \frac{\theta}{1+\varepsilon\theta} \tag{3.7}$$

where, a dimensionless temperature (θ) can be defined as:

$$\theta = \frac{E}{RT_A^2}\left(T - T_A\right) \tag{3.8}$$

and

$$\varepsilon = \frac{RT_A}{E} \tag{3.2}$$

A dimensionless distance (z) is defined by

$$z = \frac{x}{r} \tag{3.9}$$

and, a dimensionless heat generation parameter is defined by the Damkohler number given by Equation 3.1. The half-width (r) for common shapes can be seen below.

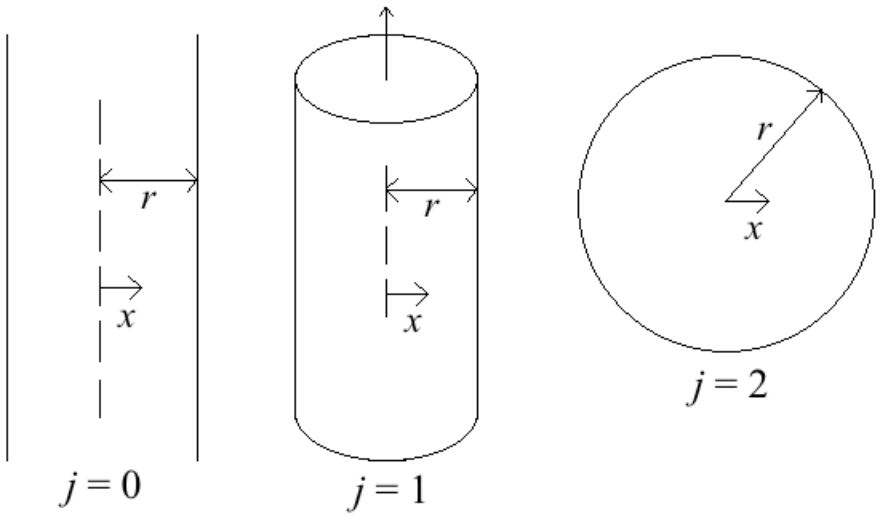

Figure 3.4: Dimensions for an infinite slab, infinite cylinder, and sphere.

Applying the given dimensionless parameters to the energy balance equation and recognizing $\varepsilon \to 0$ from Assumption 2, Equation 3.6 can be written as:

$$\frac{d^2\theta}{dz^2} + \frac{j}{z}\frac{\partial\theta}{\partial z} + \delta e^{\theta} = 0 \tag{3.10}$$

This can be thought of as the activation temperature to the system temperature. The second parenthesis represents the energy by chemical reaction to the heat conducted. It too is large for combustion substances, ~ 10^4, as δ is usually of order 1.

A solution for θ will depend on δ. As δ increases (caused by an increase in r or T_A), a value will be reached where a steady solution is not possible. This is the critical value, δ_c. Equation 3.10 can be solved for different scenarios, and the δ_c can be determined. This process is described in the following sections. Then if $\delta \geq \delta_c$ for the actual state of the substance, ignition is said to occur. Three common scenarios will be examined, and the results found in the literature will be presented.

3.3 Material in a Hot Environment

3.3.1 Finding the Critical Damkohler Number

Consider a uniform material with a given geometric shape exposed to the environment as seen in Figure 3.5.

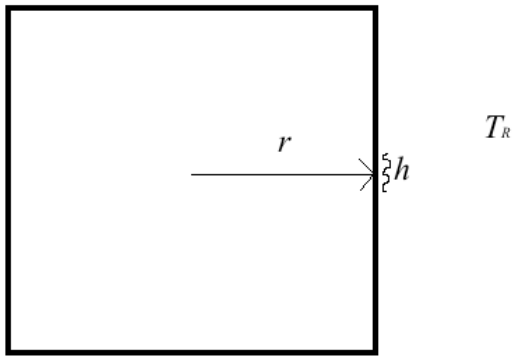

Figure 3.5: Reactive material in hot environment at T_A.

To find a solution to the Equation 3.10, boundary conditions must be added. Considering the boundary condition at the surface of the object, the heat transfer can be expressed by:

$$\dot{q}'' = h\left(T_s - T_A\right) \tag{3.11}$$

At the surface layer, the amount of convective heat transferred to the surroundings must be the same as the conduction heat transfer within the material; therefore, the surface layer may be represented by

$$-\lambda \frac{\partial T}{\partial x} = h\left(T_s - T_A\right) \tag{3.12}$$

at $x = r$. By symmetry, the boundary condition at the center is

$$\frac{dT}{dx} = 0 \tag{3.13}$$

at $x = 0$.

Finally, the boundary conditions need to be non-dimensionalized by substituting the dimensionless variables. The boundary condition are given by

$$-\frac{d\theta}{dz} = \alpha\theta \tag{3.14}$$

for the center, $z = 1$, and

$$\frac{d\theta}{dz} = 0 \tag{3.15}$$

for the surface, $z = 0$. Notice that the boundary condition for the body center is a function of the Biot number, α. The Biot number is expressed by the following equation.

$$\alpha = \frac{hr}{\lambda} \tag{3.16}$$

Examining the non-dimensional expressions, a steady-state solution will depend on α, δ, and z.

The heat transfer coefficient can be a combination of convection and radiant heating from the surroundings. For the unsteady problem where the initial material temperature $T_i < T_A$, the temperature response is illustrated for a symmetric slab of r in Figure 3.6. This case is like the "oven-method", where cubes of material are inserted into a hot oven, to find critical temperature.

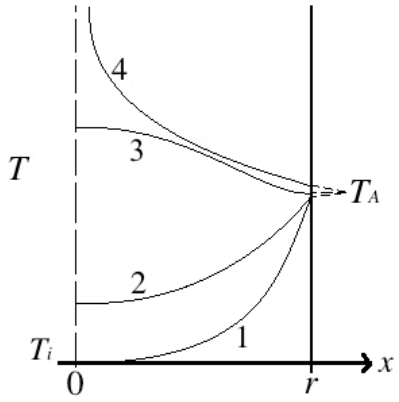

Curves 1 and 2: heating from T_A

Curve 3: steady result, now cooling to T_A, $\delta < \delta_c$

Curve 4: ignition event, $\delta > \delta_c$

Figure 3.6: Symmetric self-heating over time for an infinite slab

A solution to Equation 3.10 with boundary conditions has been given by Thomas (Thomas, 1958) for the symmetric slab. The result shows that δ_c depends on α, such that

$\alpha \to 0$, $\quad \delta_c = \frac{\alpha}{e}$

$\alpha \to \infty$, $\quad \delta_c = 0.88$

Complete results are given for the slab, cylinder, and sphere in Figure 3.7, and θ_S (θ at z =1) and θ_o (θ at $z = 0$) are given in Figures 3.8 and 3.9, respectively.

To implement these results for a given geometry, the following properties must be known: the size of the material (r), the specified ambient temperature (T_A), and the computed Biot number (α).

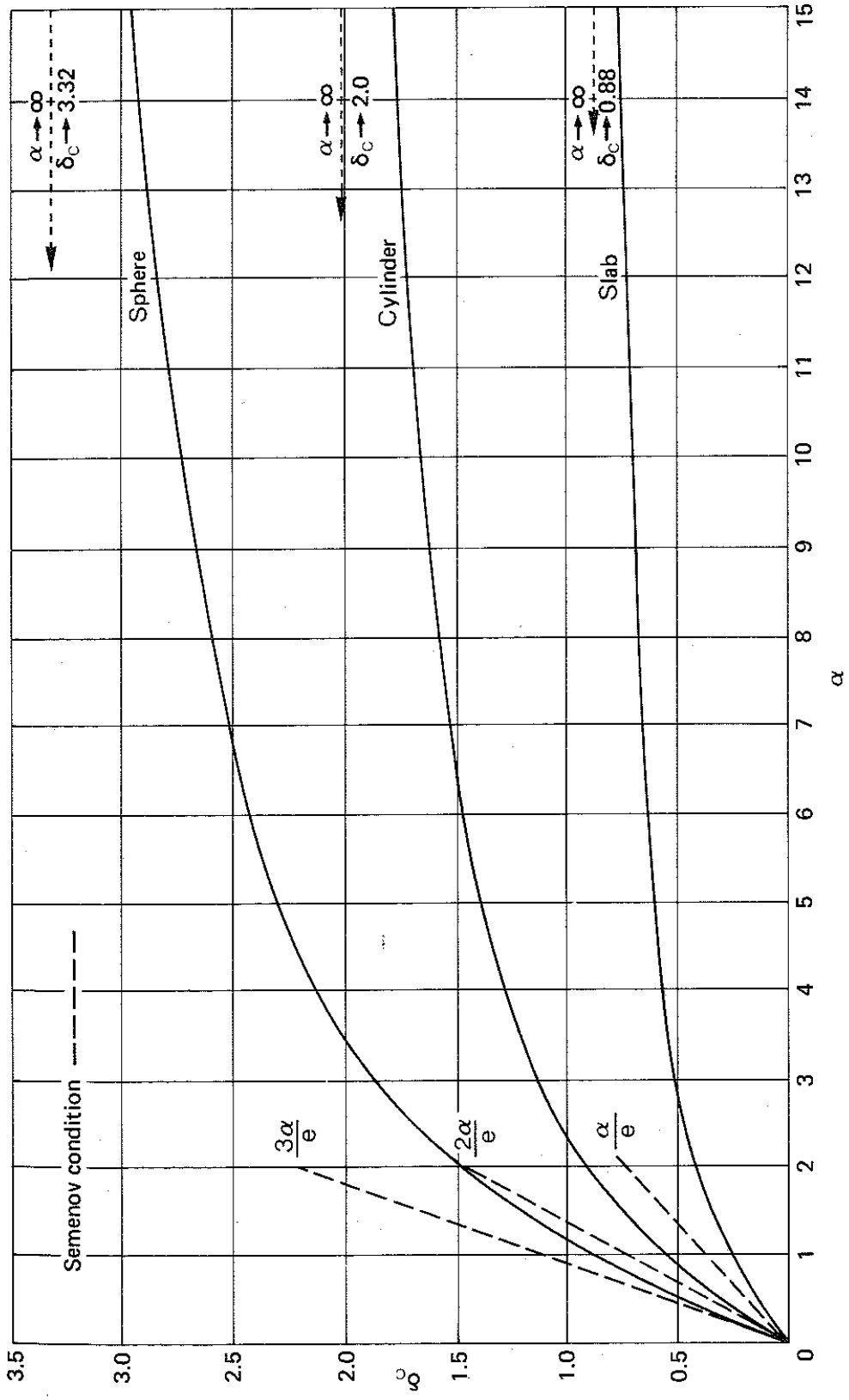

Figure 3.7: δ_c as a function of the Biot number for common shapes (Thomas, 1958)

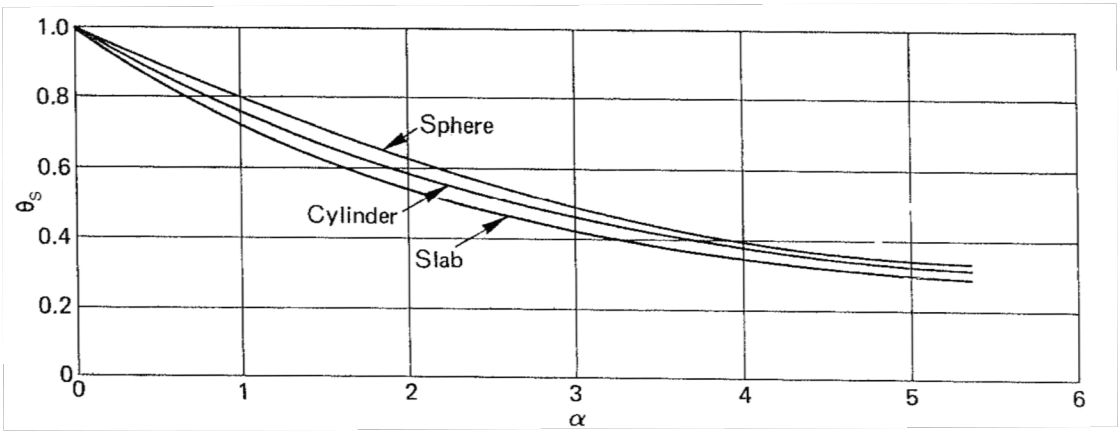

Figure 3.8: θ_S as a function of the Biot number for common shapes (Thomas, 1958)

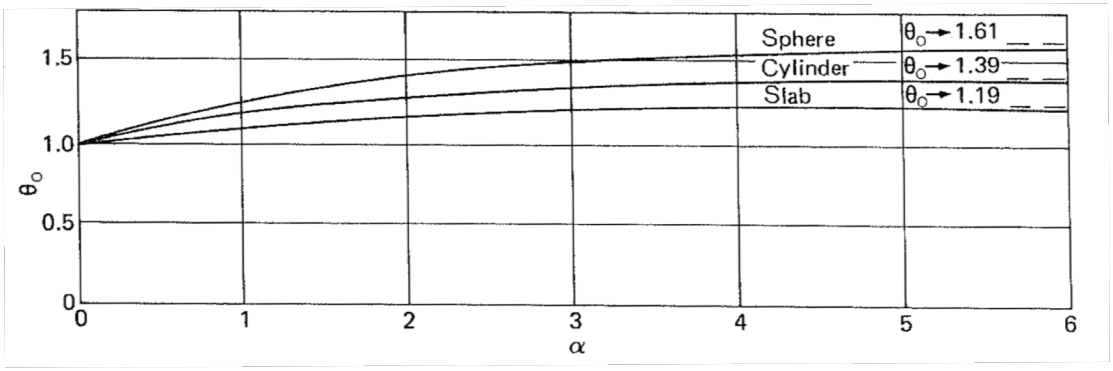

Figure 3.9: θ_o as a function of the Biot number for common shapes (Thomas, 1958)

Also, the table below gives δ_c for common shapes as listed by Bowes (Bowes, 1984). The following δ_c values listed are for cases where all assumptions are satisfied.

Body	$\delta_c(\alpha \rightarrow \infty)$	θ_o
Infinite plane slab, thickness 2r	0.878	1.119
Infinite cylinder, radius 2r	2.000	1.386
Infinite square rod, side 2r	1.700	1.492
Sphere, radius r	3.322	1.622
Short cylinder, radius r, height 2r	2.764	1.778
Cube, side 2r	2.519	1.888

Table 3.1: Values for a more complete list of geometries for $\alpha \rightarrow \infty$ (Bowes, 1984)

3.3.2 Correcting for Finite Biot Number

If certain assumptions to the self-heating theory are not met, corrections can be applied to increase the accuracy of the critical Damkohler number. The cases for which corrections may be applied are for the cases of finite Biot numbers, material consumption from the reaction, and materials involving low activation energy. Bowes uses correction equations from Barzykin et al (Barzykin, Gontkovskaya, & Merzhanov, 1966). The corrections act as factors to the uncorrected critical Damkohler value, denoted $\delta_c(\infty,0,\infty)$. The following equation may be used for corrections:

$$\delta_c(\alpha,\varepsilon,B) = \delta_c(\infty,0,\infty) C_\alpha C_\varepsilon C_B \tag{3.17}$$

where, $\delta_c(\alpha,\varepsilon,B)$ denotes the critical Damkohler number corrected for α,ε,B, and $C_\alpha, C_\varepsilon, C_B$ are the correction factors for α,ε,B, respectively. Here, C_α corrects for the Biot number, C_ε corrects for low activation energy, and C_B corrects for material depletion.

As seen in Figure 3.7, δ_c will vary significantly for small values of α. In finding the critical Damkohler number corrected for α, denoted $\delta_c(\alpha)$, the correction factor can be found with two methods. The first method is by inspection of Figure 3.7 and is valid for $0.0<\alpha<15$. The graph may be used directly to find $\delta_c(\alpha)$ for the listed shapes: sphere, cylinder, and slab. If the desire shape is not shown in Figure 3.7, the curve for a sphere may be used in the following manner. The critical Damkohler number for a sphere corrected for α, $\delta_c(\alpha)_{sphere}$, can be obtained by inspection from Figure 3.7 and divided by the uncorrected critical Damkohler number for a sphere from Table 3.1,

$\delta_c(\alpha \to \infty)_{sphere}$ [3.322]. This is the α correction factor, C_α, and may be thought of as a percentage of the α corrected and uncorrected Damkohler values of a sphere. This percentage is then multiplied with the uncorrected Damkohler number for the desire shape, $\delta_c(\alpha \to \infty)_{shape}$, found in Table 3.1, i.e.:

$$\delta_c(\alpha) = \delta_c(\alpha \to \infty)_{shape}\left[\frac{\delta_c(\alpha)_{sphere}}{3.322}\right] \tag{3.18}$$

The second method has been provided by Barzykin et al (Barzykin, Gontkovskaya, & Merzhanov, 1966) and adopted by Bowes. Barzykin offers a Biot correction correlation that similarly follows Figure 3.7. The following correlation can be used for any material shape with known finite Biot number:

$$C_\alpha = \frac{\alpha}{2}\left(\sqrt{\alpha^2+4}-\alpha\right)\exp\left(\frac{\sqrt{\alpha^2+4}-\alpha-2}{\alpha}\right) \tag{3.19}$$

where, $\delta_c(\alpha) = \delta_c(\alpha \to \infty)C_\alpha$ from Equation 3.17.

Example for Biot correction: Suppose $\delta_c(\alpha)$ for an infinite slab is to be found. If the Biot number is calculated to be 3 ($\alpha = 3$), then $\delta_c(\alpha = 3) \approx 0.5$ from the slab curve in Figure 3.7. The figure below shows the low Biot values of the slab curve and the corresponding $\delta_c(\alpha)$ values.

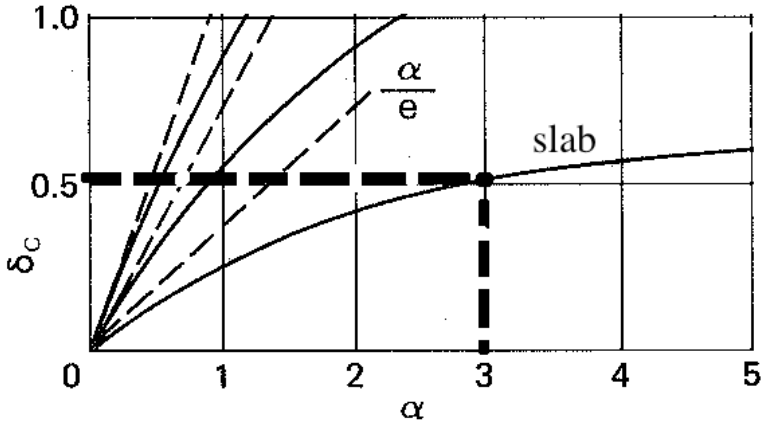

Figure 3.10: Finding δ_c for a slab with $\alpha = 3$

To test the graph using Equation 3.18, $\delta_c(\alpha \to \infty)_{slab}$ is known to be 0.88 and $\delta_c(\alpha = 3)_{sphere}$ is approximately found from Figure 3.7 to be 1.85. The equation gives $\delta_c(\alpha = 3)_{slab} \approx 0.49$ which, is very close to $\delta_c(\alpha = 3)_{slab} \approx 0.5$ value found directly from the graph. Calculating $\delta_c(\alpha = 3)_{slab}$ from Equation 3.19, $\delta_c(\alpha = 3)_{slab} \approx 0.50$.

3.3.3 Correcting for Low Activation Energy

By the assumptions under the self-heating theory, the activation energy must be high enough for the condition

$$\varepsilon = \frac{RT_A}{E} << 1 \tag{3.2}$$

to be justified. E is typically in the range of 60-140 *kJ/mol* for self-heating materials and as a result, $\frac{RT_A}{E}$ is generally on the order of $\frac{T_A}{10^4}$ ($E \sim 100$ *kJ/mol*). For fire conditions,

$T_A \sim 10^3$ yields $\varepsilon \sim 0.1$. Babrauskas suggests that corrections for low activation energy do not need to be made in practice for $E > 40$ *kJ/mol* (Babrauskas, 2003).

Under circumstances that require a correction and E is known for the material, a correction factor can be applied to the $\delta_c(\alpha \to \infty)$ from Table 3.1. Barzykin et al provide the following correction factor:

$$C_\varepsilon = 1 + \varepsilon \tag{3.20}$$

3.3.4 Correcting for Reactant Consumption

Now that the Critical Damkohler Number is corrected for the finite Biot Number and low activation energy, the Critical Damkohler Number can next be corrected for reactant consumption. The self-heating theory assumes a single zeroth order exothermic reaction generating heat as a function of temperature only. As in all real systems, reactants are consumed and thus an ideal steady state is not possible. To account for reactant consumption, it is necessary to determine the dimensionless adiabatic temperature rise for the system (B), as well as a dimensionless ambient temperature (ε). The equation for ε is given by Equation 3.2 and B can be found using the following:

$$C_B = \frac{1}{a - b\left(n/B\right)^{2/3}} \tag{3.21}$$

where a and b are constants that vary with ε and n is the reaction order.

Also,

$$B = \frac{E}{RT_A^2}\frac{QC_o}{\rho c} \tag{3.22}$$

where Q is the heat of reaction, and C_o is the initial concentration of the reactant. For porous solids, C_o and ρ will approximately be the same, and therefore, cancel each other. Values for a and b with known ε can be found from the table below.

ε	a	b
0.000	1.000	2.28
0.025	0.973	2.35
0.050	0.944	2.41
0.075	0.916	2.49
0.100	0.885	2.56

Table 3.2: a and b values with varying ε (Bowes, 1984)

Due to doubts by B F Gray and Sherrington on the validity of the analysis, Barzykin et al suggests that a = 1 and b = 2.4 can be used with reasonable accuracy for first order reactions, i.e. $n = 1$.

This correction is difficult to implement due to the extent of variables needed for calculations. The reaction order number (n) would need to be obtained using a detailed chemistry analysis, which is not likely feasible. Babrauskas suggests that $n = 1$ may be assumed as a rough estimate (Babrauskas, 2003). Further, Q would need to be obtained using a calorimetry method. Instead, a rough estimate will often suffice in order to gain a general understanding of the effects of reactant depletion.

3.4 Reactive Material on Hot Surface

3.4.1 Finding the Critical Damkohler Number for Unsymmetric Heating

The second scenario is for a reactive material located on a hot surface. Here the scenario has a slab of thickness $2r$ on a hot surface of temperature T_P with its other face exposed to the ambient at T_A having Newtonian cooling. Figure 3.11 shows the

arrangement, and how the temperature would behave over time when $T_i = T_A$. This case is unsymmetric since the maximum temperature (T_m) is not located in the center of the slab.

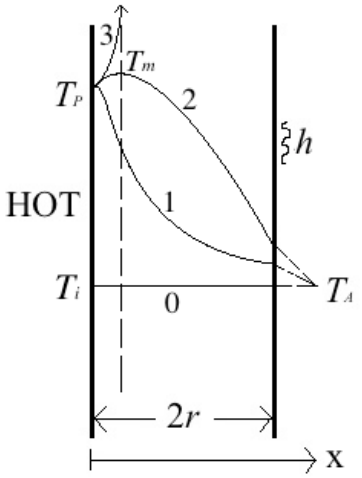

Curve 0: Initial State; $T_i = T_A$

Curve 1: Unsteady heating

Curve 2: Steady condition; $\delta < \delta_c$

Curve 3: Thermal runaways; $\delta \geq \delta_c$

Figure 3.11: Unsymmetric self-heating over time for an infinite slab

From Equation 3.10 in which the reference temperature is now T_P, Equation 3.1 is given in terms of T_P, not T_A; i.e. $\delta(T_P)$. Also, the dimensionless temperature can be rewritten in terms of T_P as seen below:

$$\theta(T) = \left(\frac{E}{RT_P}\right)\left(\frac{T - T_P}{T_P}\right) \tag{3.23}$$

The boundary conditions are

$$\theta = 0 \qquad \text{at } z = 0$$

$$-\frac{d\theta}{dz} = \alpha\left(\theta_S - \theta_A\right) \qquad \text{at } z = 2 \tag{3.24}$$

where z is the dimensionless distance from Equation 3.9. The dimensionless temperature parameter can be expressed in terms of the exposed surface temperature, θ_S for $T = T_S$, ambient temperature, θ_A for $T = T_A$, or maximum material temperature, θ_m for $T = T_m$.

In most cases, a feasible critical Damkohler number, corrected for α, can be obtained with the approximate solutions below:

$$\delta_c = \frac{1}{2}\left(\frac{\alpha}{1+2\alpha}\right)^2 \left(1.4-\theta_A\right)^2 \qquad \text{when } \alpha > 5$$

and (3.25)

$$\delta_c = -\frac{\alpha}{4e} \qquad \text{when } \alpha \to 0$$

However, a more exact result can be taken from the figure below.

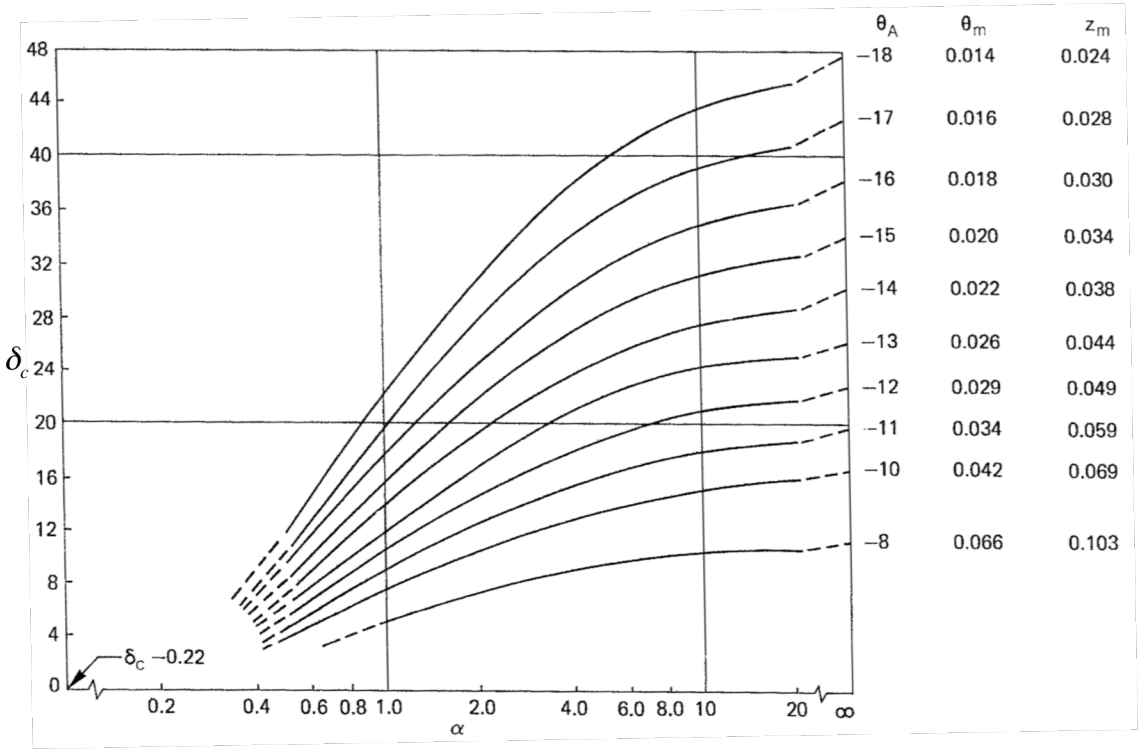

Figure 3.12: δ_c as a function of α and θ_A for an unsymmetrically heated slab (Bowes, 1984)

Additionally, Figure 3.12 gives the dimensionless maximum material temperature (θ_m) as well as its corresponding dimensionless location (z_m). Note, θ_A is negative as $T_P > T_A$. The maximum dimensionless temperature and its position are also given. For the unsymmetric case, δ_c values are much higher than the symmetric values.

There appears to be no correction correlations due to reactant consumption for an unsymmetrically heated case. However, study by Tyler and Jones identifies that there is an even stronger effect from reactant consumption for the unsymmetric case as compared to the symmetric case. For this reason, caution should be taken when analyzing an unsymmetric self-heating scenario with low B values. This is also an area that further research is suggested.

3.5 Hot Material in a Cold Environment

3.5.1 Finding the Critical Damkohler Number

Here a symmetric hot body is placed in a cooler ambient environment with Newtonian cooling at the surface. Figure 3.13 illustrates the transient behavior for an initial temperature T_i in surroundings at T_A.

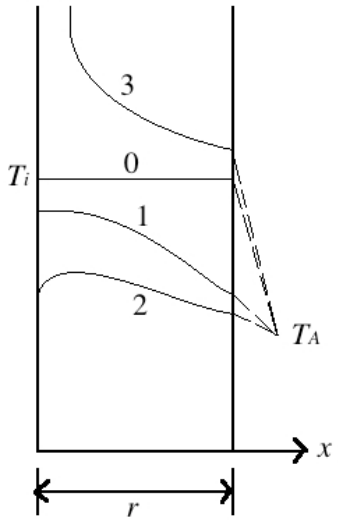

Curve 0: initial condition

Curve 1: cooling

Curve 2: steady result, $\delta < \delta_c$

Curve 3: ignition event, $\delta \geq \delta_c$

Figure 3.13: Transient behavior of hot self-heating infinite slab in cooler ambient

This is inherently an unsteady problem since the initial condition $t = 0$ and $T = T_i$ must be used. However, numerical results and an approximate solution yield the following:

$$\delta_c(j) = M_j\left[\ln(2\theta_o)\right]^{N_j} \qquad \text{when } \alpha \to \infty \tag{3.26}$$

where,

Shape	M_j	N_j
Slab (j=0)	2.66	1.30
Cylinder (j=1)	7.39	0.83
Sphere (j=2)	12.10	0.60

Table 3.3: M_j and N_j values for common shapes (Bowes, 1984)

Figure 3.14 below gives a more exact result for Equation 3.26:

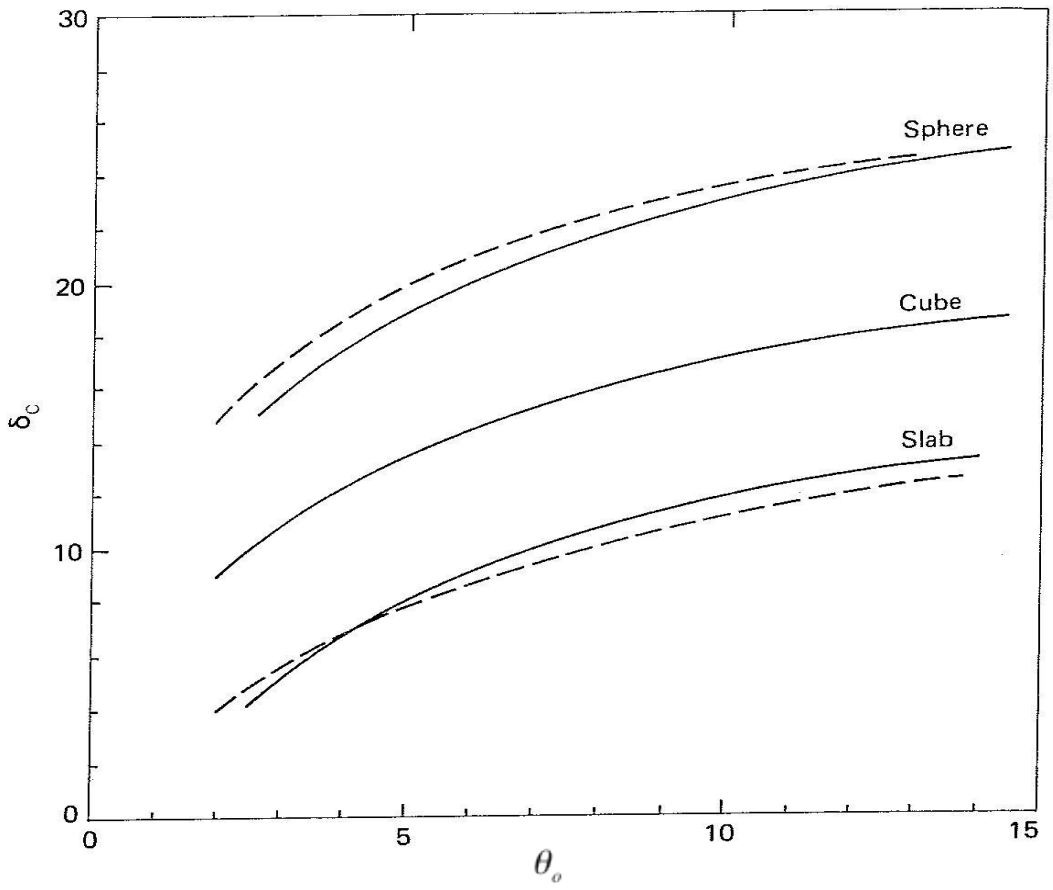

Figure 3.14: δ_c as a function of θ_o for common shapes with $\alpha \to \infty$ (Bowes, 1984)

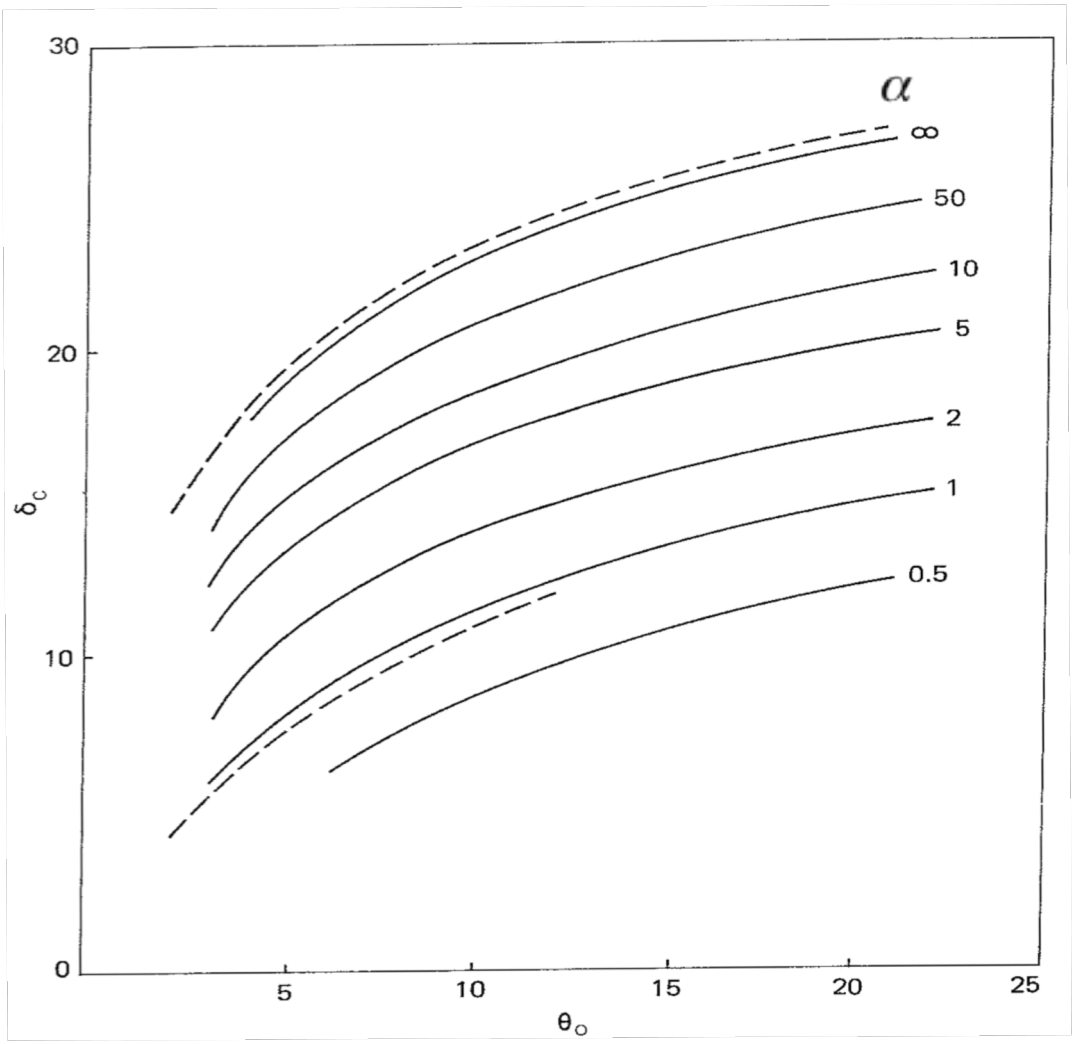

Figure 3.15: δ_c as a function of θ_o for hot spots of a sphere with varying α values (Bowes, 1984)

Also, Figures 3.14 and 3.15 showing results for $\alpha \to \infty$, and for a sphere with $0.5 \leq \alpha \leq \infty$, respectively. In addition, for arbitrary α, the approximation for the slab (j = 0), cylinder (j = 1) and sphere (j =2) is given as

$$\delta_c = \alpha(1+j)\theta_o e^{\frac{\alpha(1+j)}{\delta_c}} \tag{3.27}$$

Here the notation uses T_i as the reference, so the critical Damkohler number is written as a function of the initial temperature, i.e. $\delta_c = \delta_c(T_i)$ and, the dimensionless temperature parameter is written as:

$$\theta_o = \left(\frac{E}{RT_i}\right)\left(\frac{T_i - T_A}{T_i}\right) \tag{3.28}$$

This problem can also be transformed into a "hot spot" scenario in which a hot object of temperature T_i initially spanning a radius r over an infinite symmetrical body with remainder temperature T_A. The results for $\alpha \rightarrow \infty$ in the "hot body" scenario relate directly to θ_o for the hot spot replacing $2\theta_o$ for the hot body in Equation 3.26.

Chapter 4: *P* and *M* Properties

4.1 Introduction to P and M Properties

Many of the material properties required to find the Damkohler number may be difficult to obtain experimentally. Calorimetric methods, such as differential scanning calorimetry (DSC) and differential thermal analysis (DTA), are available to find the necessary properties. Concerns arise using these methods to find thermal properties of materials in large-scale applications since these tests use specimens many orders of magnitude less, resulting in the risk of error. It is easier and more accurate to combine the unknown properties into two material constants, *P* and *M*. These properties are desirable since they are not a function of the shape and size of the sample, unlike critical temperature. The notation and units of these properties vary in different literature so Bowes' (1984) notation and units will be used. *P* and *M* are defined below:

$$P = \frac{E}{R} \qquad [\mathrm{K}] \tag{4.1}$$

$$M = \ln\left(\frac{E}{R}\frac{\rho A Q}{\lambda}\right) \qquad \text{or} \qquad \exp(M) = \frac{E}{R}\frac{\rho A Q}{\lambda} \qquad \left[\frac{K^2}{mm^2}\right] \tag{4.2}$$

P and *M* can be substituted into Equation 3.1 to simplify the Damkohler equation in terms of *P*, *M*, *r*, and T_R as seen in the equation below:

$$\delta = \frac{r^2}{T_R^2}\exp\left(M + \frac{-P}{T_R}\right) \qquad \text{(Eq 4.3)}$$

where,

$T_R \equiv T_A$ for cold material in a hot environment

$T_R \equiv T_P$ for material on a hot surface

$T_R \equiv T_i$ for hot material in a cold environment

Examining Equations 4.1 and 4.2, it is obvious that P is directly proportional to the activation energy and M incorporates the activation energy, pre-exponential factor, density, thermal conductivity, and the heat of reaction.

4.2 Determining P and M from Oven Tests

In the case of the oven test, a cube of material is inserted into a hot oven at T_A. Conditions are sought where the center temperature of the cube increases sharply (thermal runaway). The equation of δ can be equated to the corrected δ_c for the cube in logarithmic form:

$$\ln\left[\delta_c\left(\frac{T_A}{r}\right)^2\right] = M - \frac{P}{T_A} \qquad (4.4)$$

By plotting the left-hand-side against $(1/T_A)$ for a set of data, the slope (P) and intercept (M) can be found. From this small scale data it is possible to extrapolate to larger scale conditions. This is the best way to quantitatively evaluate whether ignition is possible, i.e. $\delta \geq \delta_c$. This test will only yield good results if the chemical rate follows a zeroth order Arrhenius behavior, and as long as the Biot number is large or known for the oven. Good flow conditions in the oven are required to make α large. This is indicated by

the closeness of the cube surface temperature to T_A. Other factors can affect the accuracy of extrapolation, including the effects of melting, moisture, and maintaining the same material. However, corrections can be made to the results if the reaction rate order is not zero, and for low Biot numbers. Never the less, material values for P and M will be compiled for tested materials to provide a framework for assessing their potential for spontaneous ignition.

Example:

This is a basic example for finding P and M. No corrections will be made for this case, however, each correction is shown in the example from Section 4.3.

Beever (1988) ran oven basket tests for milk powder and found the critical ignition temperatures for cubes of size 5.0, 7.5, and 10.0 *cm*. The CAT's are listed below

Cube Size, $2r$ (*mm*)	Critical Temperature (°C ± 1 °C)
50	171
75	156
100	141.5

Table 4.1: CAT values for each milk powder oven test sample (Beever, 1988)

The uncorrected critical Damkohler value for a cube in a hot environment is 2.52 from Table 3.1. Next $\ln\frac{\delta_c T_A^2}{r^2}$, where T_A is the CAT in units of K for each basket and r is in the units of *mm*, is plotted against $1/T_A$. The data to plot is listed below in the second and third column.

Cube half-width, r (mm)	$\ln\frac{\delta_c T_A^2}{r^2}$	$1/T_A$ $[K^{-1}]$
25	6.7	2.25E-03
37.5	5.8	2.33E-03
50	5.2	2.41E-03

Table 4.2: Cube half-width, and x,y data for P and M plot

After plotting the x,y coordinates, the points are fit with linear regression to find the equation of the line. The plotted points and the corresponding linear equation can be seen below.

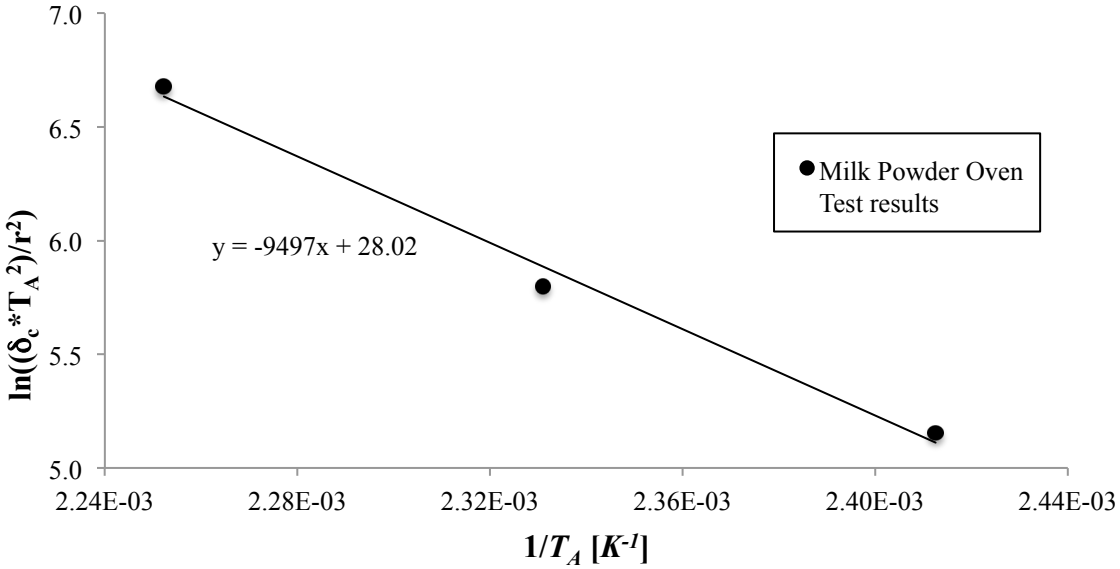

Figure 4.1: Linear regression to find P and M for milk powder

The linear equation from Figure 4.1 is y = -9,497x + 28.02. The slope of the line gives P = 9497 [K] and the y-intercept gives M = 28.02, with units based on e^M having units of K^2/mm^2. The values of P and M relate to Equation 4.3 as such:

$$\ln\frac{\delta_c T_A^2}{r^2} = 28.02 - \frac{9497}{T_A} \tag{4.5}$$

4.3 Example: Finding P and M for Wood Fiberboard

Bowes (Bowes, 1984) finds *P* and *M* values of wood fiberboard using the Frank-Kamenetskii model and the full procedure is presented below. The wood fiberboard example has information about the material is known so that all of the corrections may be implemented. Thomas (1958) and Bowes (1984) have wood fiberboard oven test results for cubes and slabs, and this data is combined with from Mitchell to increase the data set. The slabs used are of length 0.2 *m* with various thicknesses. Mitchell uses wood fiberboard cubes of width 2*r* and octagonal stacks of width and height 2*r*.

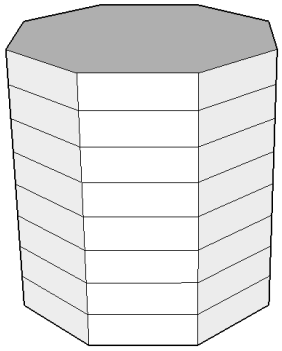

Figure 4.2: Octagonal stack of width and height of 2*r*.

The uncorrected critical Damkohler number $[\delta_c(\infty,0,\infty)]$ for the octagonal pile is calculated by Bowes to be 2.77. As expected, the octagonal pile value closely fits the value of 2.76 from a short cylinder. From Table 3.1, $\delta_c(\infty,0,\infty)$ values for the cubes and slabs are 2.52, and 0.88 respectively.

4.3.1 Varying Parameters

The half-length is needed for the calculations and is measured directly from the material size. For a circle the half-length would be half of the diameter, which is the equivalent of the radius, and would be half of the height for a square. Next, a standard basket-oven spontaneous ignition test can be used to find the critical ambient temperatures (CAT) for each pile size, which is the lowest temperature that causes ignition. Assuming the CAT falls between the highest observed non-ignition temperature and the lowest observed ignition temperature, the average of these two values are taken to ensure the accuracy of the CAT. Additionally, the thermal conductivity, thermal diffusivity, and kinematic viscosity of air are needed at the film temperature for the finite Biot correction calculations.

r = half-length [mm]

T_A = critical ambient temperature [K]

λ_f = conductivity of air at film temperature [$W/m\text{-}K$]

ν = thermal diffusivity of air at film temperature [m^2/s]

k_f = kinematic viscosity of air at film temperature [m^2/s]

Note: The units of half-length are listed in millimeters while the conductivity and kinetic viscosity are listed in meters.

	$\delta_c(\infty,0,\infty)$	r	T_A	λ_f	$g/\nu\kappa_f$
		mm	*K*	*W/mK*	m^{-3}
Cube*	2.52	3.2	523	0.040	4.3E+09
		6.4	485	0.038	5.5E+09
Octagonal Pile*	2.77	12.7	473	0.037	5.9E+09
		25.4	450	0.036	7.0E+09
		51	420	0.034	8.8E+09
		102	398	0.032	1.1E+10
		152	389	0.032	1.2E+10
Cube**	2.52	12.7	475	0.037	6.0E+09
		25.4	450	0.036	7.0E+09
		51	425	0.035	8.0E+09
Slab**	0.88	6.8	475	0.037	6.0E+09
		13.7	445	0.036	7.0E+09
		21	435	0.035	7.7E+09

* Based on tests from Mitchell
** Based on tests from Thomas and Bowes

Table 4.3: Parameters for wood fiberboard oven tests

4.3.2 Finite Biot Number Correction Factor

The experimental process of determining *P* and *M* values uses a convection fan in an oven to increase the Biot number of the sample. With high forced convection, the temperature gradient within the material increases along with the Biot number. If the Biot number is large enough, the temperature difference between the surface of the material and the ambient air remains negligible and there is no energy transfer by conduction. A large Biot number simplifies the calculations of *P* and *M* because it eliminates the need for the Biot number correction. However if the Biot number is finite, a correction needs to be applied since the material surface temperature differs from the temperature of the air. The material in this example is exposed to an environment with no wind, so the Biot number will be small.

The Biot number correction adjusts the uncorrected critical Damkohler number, $\delta_c(\alpha \to \infty)$ in Table 3.1, which will be used to determine if a material will lead to thermal runaway. Since there is no forced convection in this example, Nusselt correlations for natural convection may be used to obtain the heat transfer coefficient between the basket surface and environment. To determine the effect of natural convection on the material, the Rayleigh number is found using the equation below:

$$Ra = \frac{g}{\nu k_f} D^3 \frac{RT_A}{E} \tag{4.6}$$

where

g = gravity [9.81 m/s^2]

D = diameter = $2r/1{,}000$ [m]

R = universal gas constant [$8.31*10^{-3}$ *kJ/mol-K*]

E = activation energy [100 *kJ/mol*]

In the case of the slabs, the D used is equal to the length ($D = 0.2m$). Note, Bowes uses this equation as a practical approach to finding *Ra*. A more appropriate calculation for *Ra* is given by Equation 4.7.

Notice E is used for Equation 4.6. Bowes estimates this to be 100 *kJ/mol* for wood fiberboard. In many cases the activation energy is not known and not needed since it is found in *P*, so Equation 4.7 can be used when the surface temperature of the material is known.

$$Ra = \frac{g}{\nu k_f} D^3 \frac{T_S - T_A}{T_A} \tag{4.7}$$

Next, *Ra* is used in determining the heat transfer coefficient due to convection. In combination with the radiation component of the heat transfer, the total heat transfer to

the wood fiberboard is found. A general equation for determining the convective heat transfer coefficient (h_c) is proposed by Bowes (Bowes, 1984) and seen below:

$$h_c = \frac{\lambda_f}{D}(2.0 + 0.6Ra^{1/4}) \tag{4.8}$$

Babrauskas also recommends this equation as a practical approach for any shape since calculations for a body of arbitrary shape generally become burdensome (Babrauskas, 2003). This equation is only used for a case where free convection is the only form. In cases where forced convection is used, such as a convection oven with high fan speed, the heat transfer coefficient is most accurately found experimentally. An accurate method of determining the heat transfer coefficient in forced convection cases is described in Chapter 5. The equation for the radiative heat transfer coefficient (h_r) is:

$$h_{rad} = \frac{\sigma\left(T_S^2 + T_A^2\right)\left(T_S + T_A\right)}{\frac{1-\varepsilon_S}{\varepsilon_S} + F_{12} + \left(\frac{1-\varepsilon_O}{\varepsilon_O}\right)\left(\frac{A_{basket}}{A_{oven}}\right)} \tag{4.9}$$

where

ϵ_S = emissivity of the material surface (1 *dimensionless units*)
ϵ_O = emissivity of the surroundings (1 *dimensionless units*)
σ = Stefan-Boltzmann Constant ($5.67*10^{-8}$ $W/m^2\text{-}K^4$)
F_{12} = view factor (1.0 for parallel plates)

The surface area of the oven (A_{oven}) must be known to solve the equation. The oven area is not given in Bowes' example because he reduces the equation under the assumption of an infinite Biot number and equal surface areas. Bowes' values will still be used for this example; however, note that a more accurate estimation can be taken using Equation 4.9 in its full form.

The convective and radiative heat transfer coefficients are summed to give the total heat transfer between the atmosphere and the sample. The total heat transfer is used to find the Biot number (α) of the sample using the following,

$$\alpha = \frac{(h_r + h_c)r}{\lambda_s}$$

(4.10)

where λ_s is thermal conductivity of the sample. Bowes estimates λ_S for wood fiberboard to be 0.5 *W/m-K*. Since this example is the scenario of an initially cool object in a hot environment, the δ_c correction factor from Equation 3.19, ie:

$$C_\alpha = \frac{\alpha}{2}\left(\sqrt{\alpha^2+4} - \alpha\right)\exp\left(\frac{\sqrt{\alpha^2+4} - \alpha - 2}{\alpha}\right)$$

is used with the calculated α values for each size test sample.

	r	***Ra***	h_c	h_r	α	C_α
	mm		W/m^2K	W/m^2K		
Cube*	3.2	49	22.4	32.4	3.5	0.6
	6.4	465	14.2	25.9	5.1	0.7
Octagonal Pile*	12.7	3.8E+03	9.8	24.0	8.6	0.8
	25.4	3.4E+04	7.2	20.7	14.2	0.9
	51	3.3E+05	5.4	16.8	22.7	0.9
	102	3.0E+06	4.2	14.3	37.8	0.9
	152	1.0E+07	3.8	13.4	52.1	1.0
Cube**	12.7	3.9E+03	9.8	24.3	8.7	0.8
	25.4	3.4E+04	7.2	20.7	14.2	0.9
	51	3.0E+05	5.5	17.4	23.4	0.9
Slab**	6.8	1.9E+06	4.5	24.3	3.9	0.6
	13.7	2.1E+06	4.5	20.0	6.7	0.8
	21	2.2E+06	4.4	18.7	9.7	0.8

Table 4.4: Biot correction results for wood fiberboard tests.

4.3.3 Low Activation Energy Correction Factor

Bowes estimates E to be 100 *kJ/mol*. Though E is high enough (>40 *kJ/mol*) that no activation correction is needed, it may still be applied in the following manner. From Equation 3.2, the dimensionless ambient temperature (ε) is calculated and applied to the activation energy correction factor. The combined equation gives:

$$C_\varepsilon = 1 + \frac{RT_A}{E} \tag{4.11}$$

	r	T_A	ε	C_ε
	mm	*K*		
Cube*	3.2	523	0.043	1.043
	6.4	485	0.040	1.040
Octagonal Pile*	12.7	473	0.039	1.039
	25.4	450	0.037	1.037
	51	420	0.035	1.035
	102	398	0.033	1.033
	152	389	0.032	1.032
Cube**	12.7	475	0.039	1.039
	25.4	450	0.037	1.037
	51	425	0.035	1.035
Slab**	6.8	475	0.039	1.039
	13.7	445	0.037	1.037
	21	435	0.036	1.036

Table 4.5: Wood fiberboard low activation correction results

The activation energy is known for this specific example. However, if E is not known for the material, Bowes suggests using an iteration calculation from the P constant. In other words, calculate P and M without correcting for the low activation energy. Then determine a rough estimate of E from the calculated P using Equation 4.1.

Correct for the activation energy using the rough estimate value of *E*. Then recalculate for *P* and *M*. This iteration will be a better estimate than not correcting for ε at all.

4.3.4 Reactant Depletion Correction Factor

Next, δ_c can be corrected for reactant consumption. As in all real systems, reactants are consumed and thus an ideal steady state is not possible. To account for reactant consumption, it is necessary for to determine the dimensionless adiabatic temperature rise for the system (*B*). *B* is given from Equation 3.22 and seen again below:

$$B = \frac{E}{RT_A^2}\frac{QC_o}{\rho c}$$

The heat of reaction (*Q*) for wood fiberboard is estimated to be $3.5*10^5$ *J/kg-K* and the initial concentration (*Co*) is assumed to be equal to the density. The specific heat (*c*) of wood fiberboard was estimated by Gross and Robertson to be $1.4*10^3$ *J/kg-K*. Next, the reactant depletion correction factor (C_B) can be found using *B* and the constants *a* and *b* referenced in Table 3.2 for variation with ε. The reaction order is assumed to be 1 (*n* = 1) and reasonable results can be obtained by using *a* = 1 and *b* = 2.4 for first order reactions, so these values will be used. C_B is given in Equation 3.21 and rewritten below:

$$C_B = \frac{1}{a - b\left(n/B\right)^{2/3}}$$

The results from the equations for *B* and C_B are tabulated below.

	r	T_A	B	C_B
	mm	*K*		
Cube*	3.2	523	11.0	1.94
	6.4	485	12.8	1.78
Octagonal Pile*	12.7	473	13.4	1.74
	25.4	450	14.8	1.66
	51	420	17.0	1.57
	102	398	19.0	1.51
	152	389	19.9	1.49
Cube**	279	382	20.6	1.47
	12.7	475	13.3	1.75
	25.4	450	14.8	1.66
Slab**	51	425	16.6	1.58
	6.8	475	13.3	1.75
	13.7	445	15.2	1.64

Table 4.6: Wood fiberboard reactant consumption results

4.3.5 Finding *P* and *M*

With the correction factors for the finite Biot number, low activation energy, and reactant consumption calculated, they can be multiplied with the uncorrected critical Damkohler number to find the adjusted critical Damkohler number as in Equation 3.17:

$$\delta_c\left(\alpha,\varepsilon,B\right)=\delta_c\left(\infty,0,\infty\right)C_\alpha C_\varepsilon C_B$$

Finally, the corrected critical Damkohler number can be correlated with the critical ignition temperature by plotting the right hand side of Equation 4.4

$$\ln\frac{\delta_c T_A^2}{r^2}=M-\frac{P}{T_A}$$

against 1,000/T_A. Linear regression will result in P = slope*(-1000) and M = y-intercept.

	$\delta_c(\infty,0,\infty)$	C_α	C_ε	C_B	$\delta_c(\alpha,\varepsilon,B)$	$\frac{1{,}000}{T_A}$	$\ln\frac{\delta_c T_A^2}{r^2}$
Cube*	2.52	0.6	1.043	1.94	3.13	1.91	11.33
		0.7	1.040	1.78	3.28	2.06	9.84
Octagonal Pile*	2.77	0.8	1.039	1.74	4.02	2.11	8.63
		0.9	1.037	1.66	4.16	2.22	7.17
		0.9	1.035	1.57	4.12	2.38	5.63
		0.9	1.033	1.51	4.10	2.51	4.13
		1.0	1.032	1.49	4.09	2.57	3.29
Cube**	2.52	0.8	1.039	1.75	3.68	2.11	8.55
		0.9	1.037	1.66	3.78	2.22	7.08
		0.9	1.035	1.58	3.80	2.35	5.57
Slab**	0.88	0.6	1.039	1.75	1.02	2.11	8.51
		0.8	1.037	1.64	1.14	2.25	7.09
		0.8	1.036	1.61	1.21	2.30	6.25

Table 4.7: Wood fiberboard correction results and *P* and *M* equation components

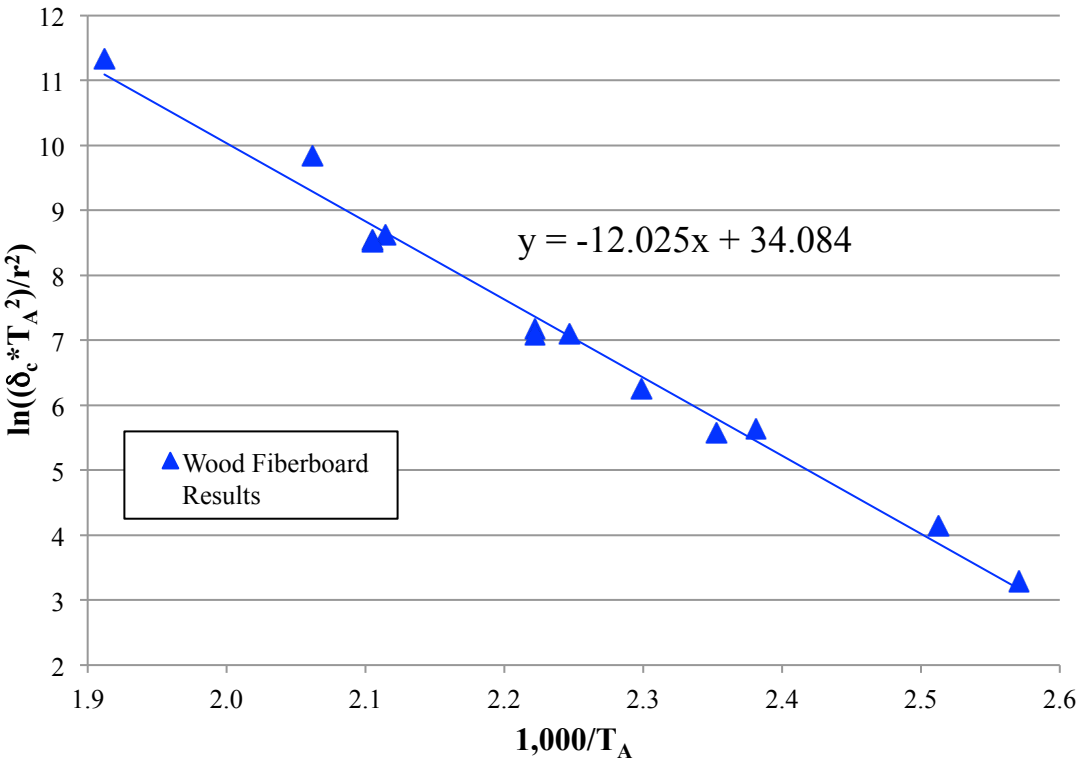

Figure 4.3: Linear regression to find *P* and *M* values for wood fiberboard

The linear regression in Figure 4.3 gives the equation y = -12.025x + 34.084. The slope of the equation is -12.025 and the y-intercept is 34.084. This means that the calculated P and M values are 12,025 K and 34.084 (with units of $e^M = K^2/mm^2$) respectively. Bowes finds the critical parameters for wood fiberboard to be M = 34.550 (with units of $e^M = K^2/mm^2$) and P = 12,145 K which is reasonably close. The small difference in values is probably due to rounding errors.

4.4 Units of M

It is important to keep the units of M consistent in studying spontaneous ignition. Bowes (1984) gives e^M in units of K^2/mm^2 and the same units are used in this thesis. Babrauskas (2003) denotes the same property (our M) as P and gives m as the unit of measure. Further, Babrauskas gives the activation energy of a material as opposed to Bowes giving P. Beever (1988) follows Bowes' nomenclature for P and M, however, gives e^M having units of K^2/m^2. The conversion from Babrauskas' and Beever's units is simply a difference of $\ln(10^6)$, as seen below:

$$M\left[\frac{K^2}{mm^2}\right]^* = M\left[\frac{K^2}{m^2}\right]^* - \ln\left(10^6\right) \tag{4.12}$$

* units seen are for e^M, not M

Example: Beever gives an M of 41.9 (e^M having units K^2/m^2) for milk powder. Subtracting $\ln(10^6)$ converts M to 28.1 (e^M having units K^2/mm^2).

4.5 List of P and M Values

Bowes (1984) and Babrauskas (2003) reference many P and M values in their literature. A list of these values has been compiled and is seen below. The units and nomenclature have been converted to those of Bowes to ensure consistency (M based on e^M having units K^2/mm^2). Some of the P and M values in the following list were calculated from the specified chemical properties from Babrauskas. See the comments column for more information about the specifics of the material.

Material	P (K)	M*	E (kJ/mol)	Comments	Source
Ammonium Nitrate	17921	43.2	149	fertilizer grade	(Hainer, 1954)
Ammonium Nitrate	16237	42.2	135	fertilizer grade with 7% additional fuel added	(Hainer, 1954)
Animal Feedstuff	8404	26.06	70		(Bowes, 1984)
Bagasse	13000	33.08	108		(Bowes, 1984)
Calcium Hypochlorite	5833	19.5	48.5	hydrated. Values are for low temperature regime	(Gray & Halliburton, 2000)
Calcium Hypochlorite	14793	44.5	123	hydrated. Values are for high temperature regime	(Gray & Halliburton, 2000)
Carbon (Activated)	10007	28.2	83.2	oven-cube tests on powdered activated charcoal over 50-190 °C temperature range	(Nelson, 1992)
Cellulose Insulation	13230	32.8	110	unretarded cellulose from adiabatic furnace test	(Issen, 1980)
Cellulose Insulation	13591	26.5	113	hot-plate method with density of 34 kg/m^3	(Ohlemiller & Rogers, 1980)
Cellulose Insulation	15876	30.1	132	insulation retarded with 20% boric acid using hot-plate method with density of 41 kg/m^3	(Ohlemiller & Rogers, 1980)
Charcoal (Activated)	11666	28.1 - 35.7	97	all types except the 3 minimally hazardous products from oven-cube tests of 10 types	(Cameron & MacDowall, 1972)
Charcoal (Activated)	12700	36.975	106	weathered	(Cameron & MacDowall, 1972)
Coal	8419	25.0	70	bituminous South African with volatile content of 26% over 120-220 °C temperature range	(Tognotti, Petarca, & Zanelli, 1988)
Cork (Dust)	13711	37.2	114	oven basket method	(Hensel, 1988)
Cork (Solid)	9622	23.9	80	calculated directly from E,Q,A, density, and conductivity from values based on small-specimen tests in adiabatic furnace	(Gross & Robertson, 1958)
Cotton	11282	28.6	93.8	based on oven-basket method on cotton fibers of $\rho = 50 kg/m^3$	(Gray, Little, & Wake, 1992)
Cotton	17319	41.4	144	calculated directly from E,Q,A, $\rho = 320 kg/m^3$, and conductivity from values based on small-specimen tests in adiabatic furnace	(Gross & Robertson, 1958)

* M based on e^M having units K^2/mm^2

Material	P (K)	M*	E (kJ/mol)	Comments	Source
Distiller's Dark Grains	8046	25.3	66.9		(Bowes, 1984)
Eucalyptus Leaves	8539	24.5	71	leaves were at density 140 kg/m^3	(Jones & Raj, 1988)
Fertilizer (12-13-6)	17319	47.9	144	based on oven-basket data for 12-13-6 fertilizer	(Huygen & Perbal, 1965)
Forest Floor Material 1	9862	27.2	82		(Jones et al, 1990)
Forest Floor Material 2	10945	30.2	91		(Jones et al, 1990)
Milk Powder	11678	26.2	97.1	skim milk from temperature range 135 – 170 °C and $\rho = 670 kg/m^3$	(Chong, Chen, & Mackerth, 1999)
Milk Powder	9502	34.7	79	skim milk from temperature range 142 – 171 °C	(Beever P. , 1984)
Milk Powder	9538	28.7	79.3	skim milk from temperature range 138 – 173 °C and density 600 kg/m^3	(O'Connor, 1990)
Milk Powder	19292	45.5	160.4	(E seems high) whole milk from temperature range 130 – 145 °C	(Chong, Chen, & Mackerth, 1999)
Milk Powder	9056	20.5	75.3	whole milk from temperature range 145 – 165 °C	(Chong, Chen, & Mackerth, 1999)
Milk Powder	9754	29.4	81.1	milk with 30% fat added from temperature range 130 – 200°C	(J.G. & Synnott, 1988)
Milk Powder	11979	34.2	99.6	milk with 44% fat added from temperature range 135 – 175°C	(Duane & Synnott, 1992)
Mineral Wool	6800	21.6	56.54		(Spokoinyi & Eidukyavicius, 1988)
Plywood (Fire Rated)	11570	35.7	96.2	calculated directly from E,Q,A, density, and conductivity for fire rated plywood	(Loftus, 1985)
Plywood (Plain)	10572	32.9	87.9	calculated directly from E,Q,A, density, and conductivity for plain plywood	(Loftus, 1985)
Rice Husks	12629	32.5	105	small scale oven-cube test with density 140 kg/m^3	(Jones & Raj, 1988)
Spent Brewing Grains	6495	19.9	54		(Walker, 1961)
Wheat Flour	15539	44.2	129.2		(Nelson, 1992)
Yeast Powder	16640	44.5	138		(Bowes, 1984)

* M based on e^M having units K^2/mm^2

Table 4.8: P and M values for specific materials

Explosive Materials

Material	P (K)	M*	E (kJ/mol)	ρ (kg/m^3)	Comments	Source
Ammonium Nitrate	26941	60.2	224		chemically pure	(Hainer, 1954)
Composition B	21649	51.6	180	1580	calculated directly from E,Q,A, with density, and conductivity	**
DATB	23333	46.9	194	1740	(2,4,6-trinitro-1,3-benzenediamine); calculated directly from E,Q,A, density, and conductivity	**
HMX	26580	57.5 – 57.8	221	1800	(octahydro-1,3,5,7-tetranitro-1,3,5,7-tetrazocine); calculated directly from E,Q,A, density, and conductivity	**
NQ	10464	29.3	87	1700	(nitroguanidine); calculated directly from E,Q,A, density, and conductivity	**
PBX 9404	26460	57.7 – 57.9	220	1800	calculated directly from E,Q,A, density, and conductivity	**
PETN	23694	57.9	197	1740	(2,2-bis[(nitrooxy)methyl]-1,3-propanediol, dinitrate); calculated directly from E,Q,A, density, and conductivity	**

* M based on e^M having units K^2/mm^2

**Original sources: (Skinner, Olson, & Block-Bolten, 1998), (Maiden, 1987), (Dobratz & Crawford, 1985); E,Q,A,ρ,λ listed by Babrauskas (Babrauskas, 2003).

Table 4.9: P and M for explosive material

4.6 Woodfiber Fire Investigation Case Study

On June 2nd, 1951, nine railcars of wood fiberboard were in transit from their manufacturer in the South, to upstate New York. While in the course of switching, only a few miles outside of their destination, one of the freight cars ignited and was left to burn. The remaining cars continued to the Army Warehouse in Voorheesville, NY, where they were unloaded into one pile exceeding 24,000 ft^3. On June 17th, two days after unloading, a fire broke out that destroyed the warehouse and its contents. Spontaneous ignition was determined to have caused the fire (Mitchell, 1951).

The Frank-Kamenetskii method was applied to determine the likelihood of spontaneous ignition as the cause. The description of the fire scenario is vague so many needed parameters have been estimated. The stacking configuration was not specified for the fire scenario so a cube was analyzed. Also, the article suspects that the fire was due to a hot material pile being introduced to a cold environment; however, this heating configuration as well as the case of a cold material in a hot environment will be compared.

The wood fiberboard may have been hot after being manufactured and stacked without cooling to a safe temperature, approximately 208 °F (Mitchell, 1951). With the addition of the hot temperatures in the South region, the boards may have been self-heating in transit to the Army warehouse. This case was analyzed with an initial material temperature (T_i) of 208 °F (369 *K*). Weather history for Albany, NY, located within ten miles of Voorheesville, showed maximum temperatures for June 16th and June 17th was 79 °F (297 *K*) on both dates so this temperature was used for T_A (Weather Underground). *P* and *M* for wood fiberboard was obtained by Bowes (Bowes, 1984) in the example

explained previously in this chapter. Bowes determined wood fiberboard properties of M = 34.550 (e^M having units K^2/mm^2) and P = 12,145 K.

In contrast, a different case was analyzed in which the boards were assumed to initially cool, and the cool material pile was introduced into a hot environment. Summer temperatures inside the warehouse may have reached higher temperatures than the outside air due to lack of warehouse ventilation. For this case, the minimum warehouse temperature require to cause ignition was calculated.

$P = 12{,}145\ K$

$M = 34.550$ (e^M having units K^2/mm^2)

$Volume = 24{,}000\ ft^3$

$\lambda_s = 0.5\ W/mK$

4.6.1 Cube Material Pile in Hot Environment

For a cube at the described volume, the height was 28.8 ft so $r = 14.4\ ft = 4396 mm$. The uncorrected critical Damkohler number for a cube in a hot environment was 2.52 from Table 3.1. This value was corrected for a finite Biot number by estimating the convective and radiative heat transfer coefficients. From Equation 4.6, P was substituted in place of R/E and combined with Equation 4.8 to yield:

$$h_c = \frac{\lambda_f}{D}\left(2.0 + 0.6\left(\frac{g}{\nu_f \kappa_f} D^3 \frac{T_A}{P}\right)^{1/4}\right) \tag{4.13}$$

This equation gave a convective heat transfer coefficient of 2.4 W/m^2K. To estimate the radiative heat transfer coefficient from Equation 4.9, an estimation of the surface

temperature and emissivity was needed. For simplification, emissivities of 1 were used for the wood fiberboard and surroundings. For a general estimation of the radiative term, T_S was assumed approximately equal to T_A. With these assumptions, h_r was approximately 6.9 W/m^2K. Inputting the heat transfer coefficients into the Biot number equation (Equation 4.10) gave a Biot number of 818. This value was large, mainly since r was large, and showed that the Biot correction was not needed for this case.

The activation energy (E) was calculated from P in Equation 4.1 to be 101 kJ/mol. This activation energy was high enough so that the low activation energy correction was not necessary; however, a comparison in critical ambient temperature with and without the correction was made. Substituting P into Equation 3.2 and combining the equation with Equation 3.20 gave the following correction for low activation energy:

$$C_\varepsilon = 1 + \frac{T_A}{P} \tag{4.14}$$

Here, C_ε was calculated to be 1.03.

The uncorrected critical Damkohler number for a cube was 2.52 from Table 3.1. Applying the low activation energy correction factor using Equation 3.17 gave the critical Damkohler number corrected for ε to be 2.58. $\delta_c(\varepsilon)$ was compared to the Damkohler number for the pile and ignition would have likely occurred if $\delta > \delta_c$.

The Damkohler number for the stack of wood fiberboard was found using Equation 4.3, i.e.:

$$\delta = \frac{r^2}{T_R^2}\exp\left(M + \frac{-P}{T_R}\right)$$

where T_R for this case was T_A [K]. The critical ambient temperature was found such that $\delta/\delta_c = 1$, i.e. when $\delta = 2.58$ for the corrected case or $\delta = 2.52$ for the uncorrected case. Here, the CAT was found to be 106.3 °F with the low activation energy correction, and 106.0 °F without the correction. Notice, the correction in this case only changed the CAT by 0.3 °F, which was relatively small. Hence, no corrections were necessary for this example. If the temperature inside the Army Warehouse were in excess of 106 °F spontaneous ignition would have been likely. With the outside air reaching temperatures of 79 °F the warehouse may have been even hotter. Temperature data inside the warehouse would have needed to be taken to find out if these values were possible. Also, the material stack could have been larger than the estimated 24,000 ft^3. Scaling to large-scale applications is not exact. The critical ambient temperature of 106 °F was only a rough estimate and temperatures slightly lower than this value could indeed cause ignition. Hence, use of the Frank-Kamenetskii method should be used cautiously. If the warehouse temperature were 79 °F like the outside temperature, $\delta/\delta_c \approx 0.16$ and spontaneous ignition due to a cold body in a hot environment would not be likely.

4.6.2 Hot Cube Material Pile in Cold Environment

To analyze if spontaneous ignition occurred as a result of a hot material pile being introduced to a colder environment (Section 3.5), the dimensionless center temperature was calculated by substituting P into Equation 3.28 to give the following:

$$\theta_o = \left(\frac{P}{T_i}\right)\left(\frac{T_i - T_A}{T_i}\right) \tag{4.15}$$

where, T_A = 79 °F. The initial temperature of the material could have been as hot as 208 °F when stacked from the manufacturer, so this value was used for T_i. θ_O was calculated to 6.4. Figure 3.14 was used with $\theta_O = 6.4$ to find a critical Damkohler value of 14.5, i.e $\delta_c \approx 14.5$. The Damkohler for the wood fiberboard stack was found using Equation 4.3 to be 716. This gave $\delta/\delta_c = 49$ which is much higher than the critical ratio of 1. If the boards were at an initial temperature of 208 °F when stacked, ignition in the Army Warehouse for a cube shape pile size of 24,000 ft^3 would be extremely likely.

Chapter 5: Heat Transfer in Oven Tests

It is important to correct the critical Frank-Kamenetskii parameter if the material is under conditions of a finite Biot number. As part of the equation for the Biot number, seen again below,

$$\alpha = \frac{hr}{\lambda} \tag{3.16}$$

the heat transfer coefficient (h) between the material and surroundings is needed. Several methods have been developed where the heat transfer coefficient can be found experimentally, however, a new experiment will be proposed that is easy to implement and accurate for oven basket tests with wire-mesh baskets.

O'Conner (1990) developed a way of calculating the heat transfer to the center of a smooth surfaced hollow aluminum sphere. A sphere is theoretically convenient since it allows the use of direct Nusselt calculations to verify results; as opposed to a cube, which is not a common shape for direct calculations. Further, the smooth surface made direct calculations easier, since a rough mesh surface would yield different results. The method calculated the heat transfer distribution over time by tracking the center temperature. His results consistently showed the average heat transfer coefficients for aluminum spheres, at ambient temperature 143.2 °C and diameter ranging between 1.5 to 4 inches, were approximately 19 to 22 W/m^2K (O'Connor, 1990). Though the method seems valid for the smooth surface aluminum, the method would not be applicable for a wire-mesh basket since the forced hot air and radiation from the oven would easily pass through the mesh openings.

Jones and Wade (1999) developed a way to find the Biot number of for mesh oven test baskets by insulating the baskets with an inert material, glass fiber at density 146 kg m^{-3}, and measuring the center temperature. This method does in fact find the Biot number for the basket with the glass fiber; however, the thermal conductivity of the glass wool will typically differ from the conductivity of spontaneously combustible materials. This method requires the thermal conductivity of the glass fiber be known in addition to the conductivity of the testing material. Further, the method does not directly find the heat transfer coefficient at the surface of the container.

An article in the Journal of Food Engineering by Carson et al (2006) describes four methods of measuring the heat transfer coefficients within a convection oven. The aim of the study was to produce meat with desirable sanitation, color, texture, smell, and taste while minimizing weight loss during the cooking process. Cube plaster specimens, wet and dry, were used to simulate the moisture loss of a batch of meat. The first method of determining the heat transfer coefficient was to back-calculate the heat transfer coefficient from transient temperature-time data (Carson, Willix, & North, 2006). The oven temperature consistently fluctuated a difference of roughly 20 °C, which made the method invalid.

The second method of determining heat transfer coefficients by Carson was through a mass-loss-rate calculation, which measured the weight of the plaster samples throughout the heating process. The method yielded reasonable heat transfer coefficient results that ranged between 22 and 28 W/m^2K for oven temperatures between 43.6 and 134 °C (Carson, Willix, & North, 2006). The application of this method for spontaneous ignition would not be desirable since the internal heat generation from the chemical

reaction may result in higher mass-loss-rates and show inaccurate higher heat transfer coefficients than actually exist.

The next heat transfer coefficient calculation was a direct measurement of the heat flux using heat flux sensors. This method was the easiest to implement and gave h values between 15 and 40 W/m^2K (Carson, Willix, & North, 2006). These values seem reasonable; however for oven basket testing, the emissivity and texture of the heat flux sensor would differ than the mesh baskets. The difference between the sensor and basket would most likely yield inaccuracies since the heat flux sensor's smooth surface may show lower heat transfer coefficients compared to the rough basket surfaces.

The last method Carson implemented for finding the heat transfer coefficient was through direct empirical correlations based on the velocity and geometry of the samples. Direct empirical correlations were assumed laminar flow from the fan velocities; however, the geometry of the oven and fan mixing action likely created turbulent flow rendering the method invalid since the small velocities yielded negative values for the mixed condition correlation (Carson, Willix, & North, 2006).

Another article published in the Journal of Food Engineering by Melike Sakin et al (Sakin, Kaymak-Ertekin, & Ilicali, 2009) describes two additional methods of calculating the heat transfer coefficients inside of a convection oven. The methods were "Lumped Capacity" and "Time-Temperature Matching". Both methods used solid aluminum cylinders so that the low thermal conductivity of the metal may be neglected, and the temperatures at the radial axis and half radial positions were measured. The Lumped Capacity method was easy to implement and yielded reasonable results with h values of 28-34 W/m^2K with fan, and 11-20 W/m^2K without fan. The Time-

Temperature Matching also yielded similar results with values of 24-31 W/m^2K with fan and 10-21 W/m^2K without fan; however, computer programming in Visual Basic was required to solve the Gauss elimination matrix systems. Similar to the smooth surface of the heat flux gauge in the heat flux method, the aluminum cylinders would not be desirable for calculating the heat transfer coefficient in the spontaneous ignition tests since the surface differs greatly from the mesh baskets.

It is evident that calculating the heat transfer coefficient has proven challenging and there is no standard method yet available. In finding h for the application of spontaneous ignition oven tests, it is recommended to use the same stainless steel wire-mesh baskets that will be used in the oven test to ensure similar emissivities and roughness factors. The purpose of the following experiment is to provide a simple method of accurately determining the heat transfer coefficient between the convection oven and sample baskets used in oven tests.

5.1 Experimental Preparation

5.1.1 Testing Oven

The heat transfer coefficient is needed for the correction factor in determining the criticality spontaneously ignitable materials in a standard oven test. Bowes (1984) describes a standard for the oven test that can be used to find the critical ignition temperatures of spontaneously combustible materials. To ensure accuracy between critical temperature tests and heat transfer determination, the experimental setup for the oven and baskets was designed according to the standard. The oven used in this

experiment was a Memmert UFE 500 115V forced air controlled convection oven that was fitted with four type K thermocouples to measure the temperature at various locations within the oven. The internal dimensions were as follows:

Internal oven width = 0.56 *m*

Internal oven height = 0.47 *m*

Internal oven depth = 0.40 *m*

This oven was desired since it provided a uniform temperature distribution and temperature controll within ± 1 °C or better. The thermocouples were attached to a multichannel temperature-recorder so that all temperatures were taken simultaneously. Since it was desired that the test samples were suspended near the center of the oven, a 7" stainless steel rod was cantilevered to the back of the oven that provided a hanging location for the test baskets. Additionally, a nitrogen temperature controlled fire suppression system was installed as a safety device.

5.1.2 Sample Containers

Following Bowes description of assembling testing baskets for spontaneous ignition burn tests, open-topped cube containers were made using 60-mesh stainless steel wire gauze (Bowes, 1984). The cube sizes were 2.5, 5.0, 7.5, 10.0, and 15.0 *cm* long and spot welds were used to hold the shape of the baskets. To prepare the baskets for the heat transfer tests, the baskets were insulated internally to minimize heat transfer occurring inside the baskets. A layer of aluminum foil was added to the internal surface of each basket to insulate the center of the basket from forced convection and radiation heat transfer. Next each basket was filled with low-density kaowool to create an approximate

still air boundary, and a thermocouple was inserted into the center to record the center temperature. The tops of the baskets were covered with a sheet of aluminum foil, and a thermocouple was affixed to the surface of the basket to record the surface temperature.

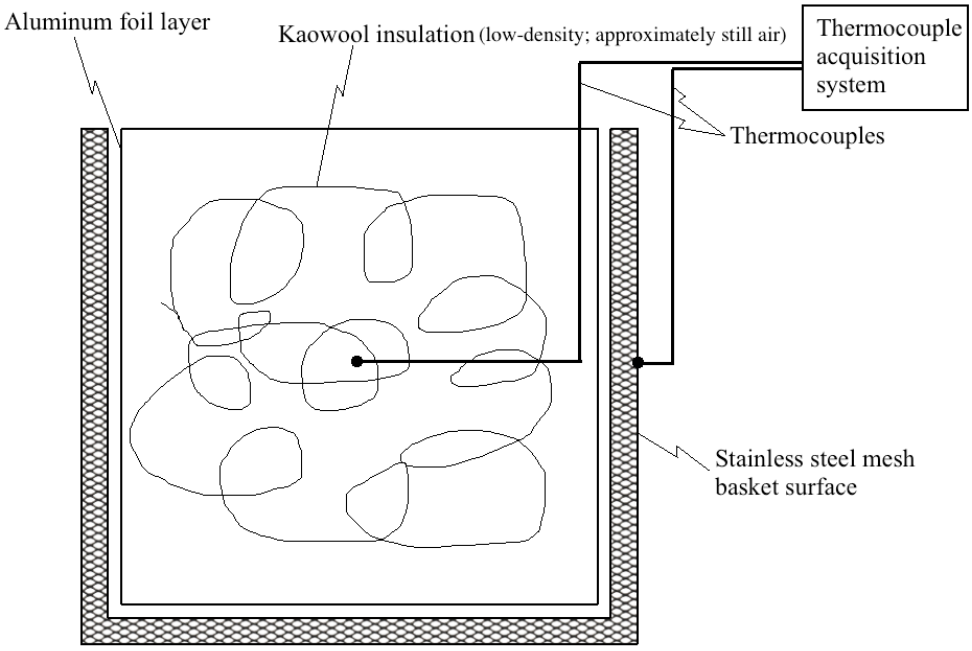

Figure 5.1: Experimental setup for heat transfer tests

5.2 Experimental Method

5.2.1 Measuring the Overall Heat Transfer Coefficient of the Baskets

The internal air velocity at the center of the convection oven was measured using an anemometer with the oven set to 20 °C and the fan speed set to max. The convection oven was then preheated to 100 °C with the fan set to maximum speed. A prepared insulated basket was quickly placed in the heated oven, careful to minimize the amount of heat that escaped from the oven. The surface and center temperatures of the basket

were recorded over time. This method was repeated for three additional scenarios listed in Section 5.2.2.

5.2.2 Experimental Configurations

1. Stainless steel (SS) surface basket placed in a stainless steel surfaced oven with maximum fan speed.
2. Stainless steel surface basket placed in a stainless steel surfaced oven with fan turned off.
3. Aluminum foil (AL) covered basket placed in an aluminum foil lined oven with maximum fan speed.
4. Aluminum foil covered basket placed in an aluminum foil lined oven with fan turned off.

The first configuration used the insulated basket with the stainless steel mesh surface exposed. The convection fan was turned to maximum speed so that the heat transfer was largely due to the combination of forced convection and radiation heat transfer. The second configuration was the same oven and basket setup; however, the fan was turned off yielding the heat transfer predominantly due to radiation and natural convection.

For configurations 3 and 4, the insulated baskets were lined with an external layer of aluminum foil; similarly, the oven's internal surfaces were lined with aluminum foil. Since aluminum foil had a much lower emissivity than the stainless steel, 0.04 (Kreith & Bohn, 2001), the aluminum foil lining minimized the amount of radiation transmitted to and absorbed into the stainless steel baskets. The aluminum-lined configurations drastically reduced the emissivity of the oven and basket, which simulated a low radiation

allowing convective heat flux to dominate the heat transfer equations. Configuration 3 used the aluminum foil oven and basket lined surfaces with the fan turned on, while configuration 4 had the fan turned off.

5.3 Calculations

5.3.1 Heat Transfer to the Basket Surface

The energy balance equation of the insulated stainless steel basket is required to derive the basket heat transfer equations. Equation 5.1 shows the energy balance equation for the stainless steel basket under the condition that the center temperature remains approximately the initial temperature, $T_{center} \approx T_{initial}$

$$mc\frac{dT_S}{dt} = hS(T_A - T_S) - \dot{q}"_l S \tag{5.1}$$

where S is the surface area of the basket ($5H^2$), m is the mass of the basket, c is the specific heat of the basket, T_S is the basket surface temperature, T_A is the oven temperature, $\frac{dT_S}{dt}$ is the rate of temperature rise of the basket surface.

For a semi-infinite solid, since the basket is thermally insulated, the surface heat flux at a constant surface temperature is given by

$$\dot{q}"_l = \frac{\lambda(T_S - T_i)}{\left[\pi\left(\frac{\lambda}{\rho c}\right)t\right]^{1/2}} \tag{5.2}$$

where λ is the thermal conductivity, and ρ is the density of air since the insulation is treated as such. From Equation 5.2, the basket-air interface can be written as

$$\dot{q}"_l \approx \frac{(T_S - T_i)}{\pi t^{1/2}}[(\lambda\rho c)_{air}]^{1/2} \tag{5.3}$$

therefore Equation 5.1 can be rewritten as

$$h \approx \frac{mc}{S}\frac{\left(\frac{dT}{dt}\right)}{\left(T_A - T\right)} + \left(\frac{T - T_i}{T_A - T}\right)\left[\frac{\left(\lambda\rho c\right)_{air}}{\pi t}\right]^{1/2} \tag{5.4}$$

for up to t @ $T_o > T_i$.

Examining the limit at $t = 0$ for the heat loss term, L,

$$\lim_{t\to 0} L \equiv \int_{t\to 0} -\left(\frac{\lambda\rho c}{\pi}\right)^{1/2}\left(\frac{T_S - T_i}{T_S - T_\infty}\right)\frac{1}{\sqrt{t}} = \frac{0}{0} \tag{5.5}$$

$$= -\left(\frac{\lambda\rho c}{\pi}\right)^{1/2}\left(\frac{\frac{dT}{dt}}{\frac{T_S - T_A}{2}t^{\frac{1}{2}} + \frac{dT}{dt}t^{1/2}}\right)$$

$$= \frac{-\left(\frac{\lambda\rho c}{\pi}\right)^{1/2}\left(\frac{dT}{dt}\right)_i}{\infty} \to 0 \text{ as } \left(\frac{dT}{dt}\right)_i > 0$$

therefore, the total heat transfer coefficient at the surface of the basket reduces to

$$\boxed{h_{tot} \approx \left[\frac{(mc)_{AL} + (mc)_{SS}}{S}\right]\frac{\left(\frac{dT_S}{dt}\right)_i}{(T_A - T_i)}} \tag{5.6}$$

where mc is known for the aluminum foil layers and stainless steel baskets.

A graphical representation of the expected temperature readings for the basket surface, basket center, and oven temperature can be seen below. Since the basket surface is exposed, the initial rise of the temperature should be steep and gradually reach the oven temperature. The insulated center of the basket should remain constant until the insulation is slowly heated. The described energy balance is only valid for the period of time that the basket center remains approximately constant. The temperature of the oven should remain approximately constant throughout the experiment.

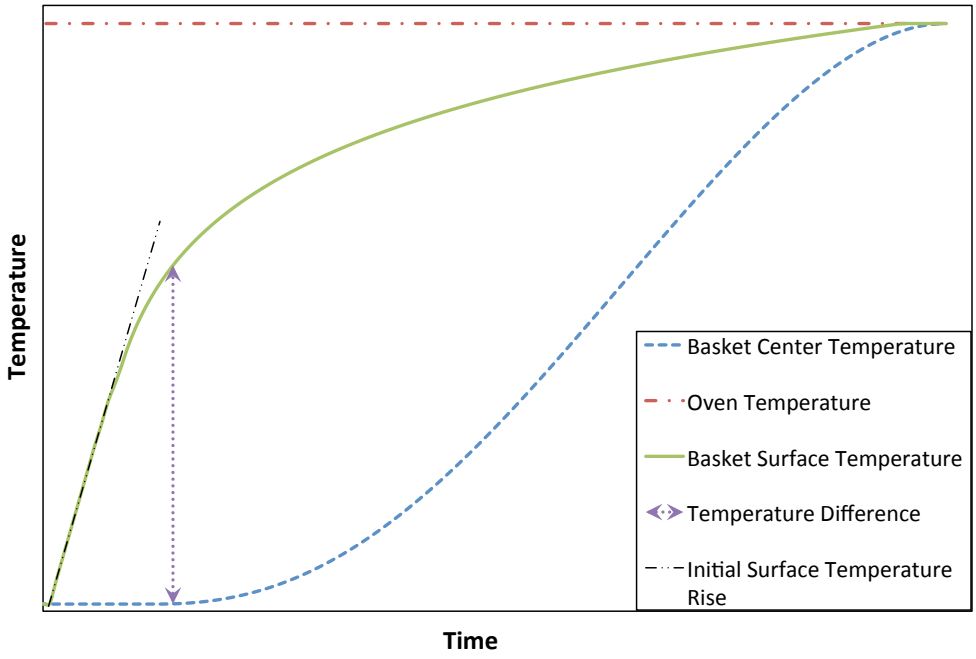

Figure 5.2: An ideal depiction of the basket surface, basket center, and oven temperatures are graphed from the heat transfer experiment.

Equation 5.6 shows the total heat transfer coefficient, which includes convection and radiation. The contributions of the convective and radiative heat transfer relate to the total heat transfer with the equation

$$h_{tot} = h_c + h_r \tag{5.7}$$

where h_c is for convection and h_r is for radiation. The radiation portion can be calculated using

$$h_{rad} = \frac{\sigma\left(T_S^2 + T_A^2\right)\left(T_S + T_A\right)}{\frac{1-\varepsilon_S}{\varepsilon_S} + F_{12} + \left(\frac{1-\varepsilon_O}{\varepsilon_O}\right)\left(\frac{A_{basket}}{A_{oven}}\right)} \tag{5.8}$$

where σ is the Stefan-Boltzmann constant ($5.67*10^{-8}\ W/m^2K$), ϵ_S is the emissivity of the basket surface, ϵ_O is the emissivity of the oven surface, F_{12} is the view factor (1.0 for parallel plates), and A_{oven} is the internal surface area of the oven.

5.3.2 Applicable Nusselt Correlations

Classical heat transfer correlations do not apply directly to a cube shape. Studies have been conducted that use computer simulation to illustrate flow around a cube; however, there seems to be no studies directly related to a cube where equal air mixing is occurring at each surface. Instead, an approximate estimation may be obtained by applying correlations for a flat plate or a sphere. The first equation analyzed is the ratio of the Grashof number to the Reynolds number squared. This ratio will determine if the convection at the surface of the cube is primarily forced, natural, or mixed. The relation of natural and forced convection is given by the equation

$$\frac{Gr}{Re^2} = \frac{[g\beta H^3(T_S - T_\infty)]/{\nu_{air}}^2}{\left(\frac{u_\infty H}{\nu_{air}}\right)^2} \tag{5.9}$$

where g is the acceleration due to gravity (9.81 m/s^2), β is the volumetric thermal expansion or the inverse of the film temperature, H is the cube height, ν_{air} is the kinematic viscosity of air at T_{film}, and u_∞ is the measured air velocity in convection oven. If Equation 5.9 is less than 0.7, then convection is essentially due to forced convection; if greater than 10, convection is essentially free convection. Values in-between 0.7 and 10 indicate that there are mixed conditions (Kreith & Bohn, 2001).

Knowing the essential convection type allows the simplification in the determination of the Nusselt correlations for an individual specimen. When different size specimens are used, as with this experiment, it may be easier to find the Nusselt number for forced and free convections for each size and combine them according to the equation

$$Nu^n{}_{combined} = Nu^n{}_{forced} \pm Nu^n{}_{natural} \tag{5.10}$$

where the sum applies to flows in the same direction, and subtraction applies to flows in opposite directions (Kreith & Bohn, 2001). Since the flow direction of the mixing air in the oven is unknown, a maximum and minimum value for the combined Nusselt number can be obtained by using the sum and subtraction. The *n* value of 3 is recommended for vertical plates.

Typical velocity values in a convection oven will require use of laminar correlations to find the Nusselt numbers for the baskets. The average surface Nusselt number for laminar flow over a sphere in a stirred bath can be calculated using

$$Nu = 2.0 + 0.6Pr^{1/3}Re^{1/2} \tag{5.11}$$

as provided by Bowes (Bowes, 1984). For parallel laminar flow over a flate plate, the average surface Nusselt number can be found using the equation below (Incropera).

$$Nu = 0.664Pr^{1/3}Re^{1/2} \tag{5.12}$$

The Nusselt correlation equivalent for a laminar natural convection to a sphere in a stirred bath is given by:

$$Nu = 2.0 + 0.6Pr^{1/3}Gr^{1/4} \tag{5.13}$$

as provided from Bowes (Bowes, 1984). The laminar natural convection to a vertical surface can be obtained using (Incropera):

$$Nu = 0.59\left(\mathrm{Gr}\,\mathrm{Pr}\right)^{1/4} \tag{5.14}$$

The heat transfer coefficient can be found from:

$$h = Nu\frac{\lambda_f}{L} \tag{5.15}$$

Care must be taken when using the previous Nusselt correlations in oven testing since the cube shape of the oven and mesh surface of the basket may result in unexpected turbulence.

5.4 Results from Heat Transfer Tests

5.4.1 Heat Transfer Coefficients

The air velocity at the center of the oven was found to be 1.6 *m/s* with the fan set to maximum speed. The temperature of the oven, basket center, and basket surface was collected for each configuration in 5.2.2 for basket sizes of 2.5, 5.0, 7.5, 10.0, 15.0 cm in height. The heat transfer coefficient of each run was calculated from Equation 5.6 and the results are tabulated below for each configuration.

	Max Fan Speed			Fan Off	
	SS Basket and Oven		AL Lined Basket and Oven	SS Basket and Oven	AL Lined Basket and Oven
Basket Width, $2r$ (cm)	h (W/m^2K)	Stand Dev	h (W/m^2K)	h (W/m^2K)	h (W/m^2K)
2.5	118.1	11.6	25.7	7.9	5.2
5	50.8	8.1	16.5	6.5	3.7
7.5	28.3	7.0	8.9	5.6	2.9
10	23.4	2.5	6.4	5.3	2.3
15	31.2	0.3	6.8	4.5	2.1

Table 5.1: h_{total} for various basket sizes and configurations at 100 °C.

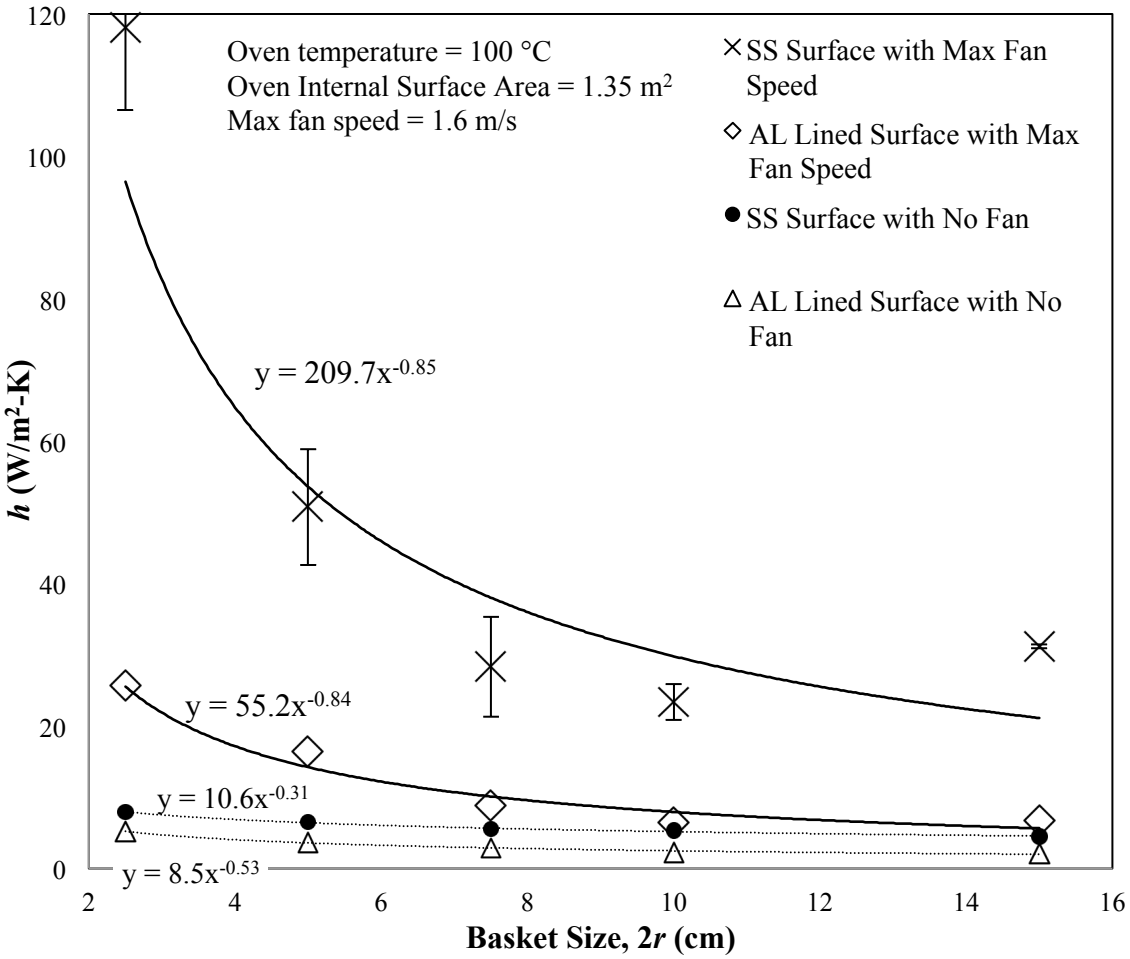

Figure 5.3: Experimental *h*'s for each configuration and basket size

5.4.2 Estimation of the Radiative Heat Transfer Coefficient

The emissivity of the aluminum foil, 0.04 (Kreith & Bohn, 2001), was used to estimate the radiative heat flux for the low radiation experiments. Using Equation 5.8, the radiative heat transfer coefficient was calculated to be 0.3 W/m^2K at 100 °C. Following Equation 5.7, the value of the radiative heat transfer coefficient was subtracted from the total heat transfer coefficient as found from the experiments using the aluminum foil to find the heat transfer coefficient due to convection.

ϵ_{AL} = emissivity of aluminum foil = 0.04 (Kreith & Bohn, 2001)
ϵ_{SS} = emissivity of stainless steel ≈ 0.22 (Incropera)

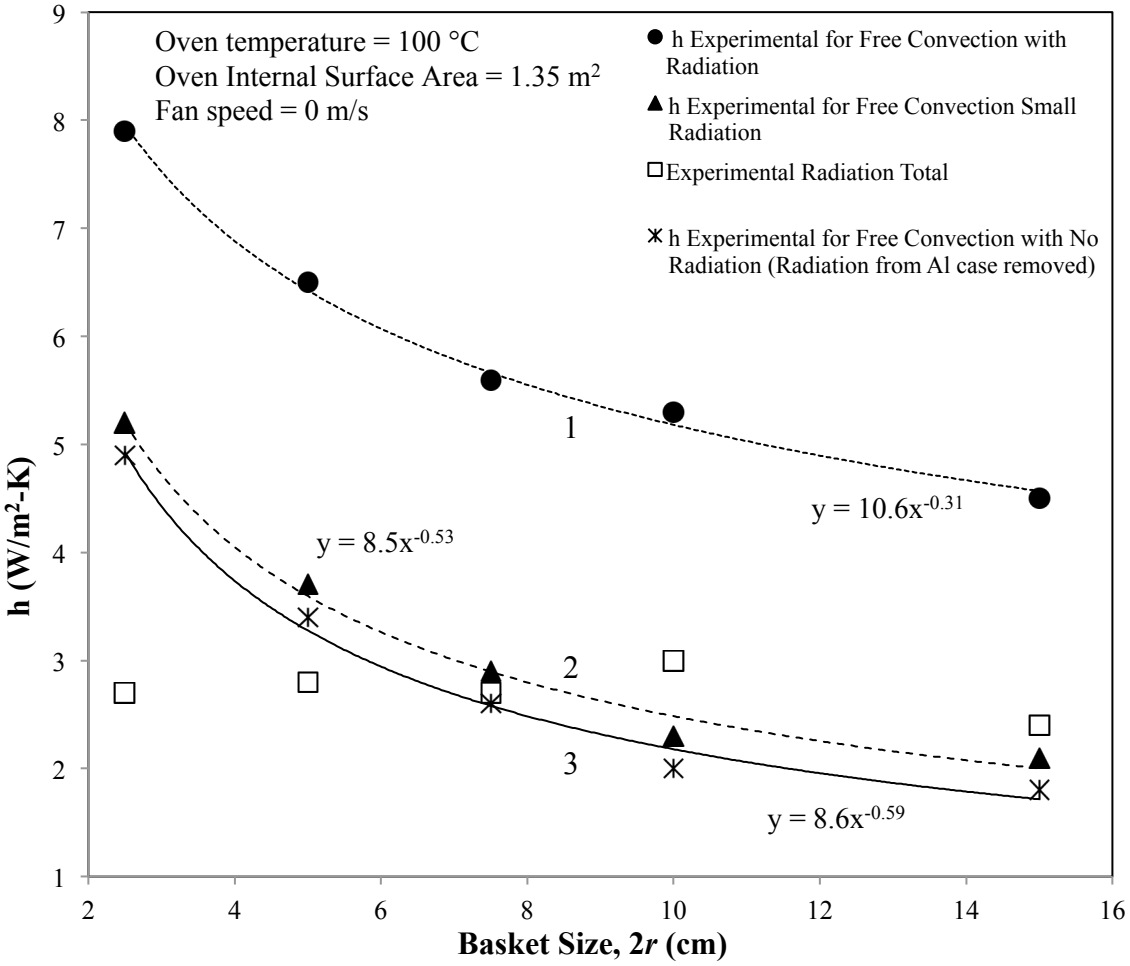

Figure 5.4: The difference between the stainless steel and aluminum surfaces for the natural convection experiments yielded a radiation difference of 2.7 W/m^2K.

Analyzing the two experiments without the fan, the free convection heat transfer for the stainless steel surface baskets was assumed to be the same for the aluminum surface baskets. This assumption allows us to find the radiation heat transfer coefficient for the stainless steel baskets using Equation 5.7. With a radiation difference of 2.7 W/m^2K between the stainless steel (curve 1 in Figure 5.4) and aluminum (curve 2 in

Figure 5.4) natural convection experiments, the radiation calculated previously for the aluminum experiments of 0.3 W/m^2K summed to the 2.7 W/m^2K yielded a total radiative heat transfer coefficient of 3.0 W/m^2K. Further, the emissivity of the stainless steel oven walls was assumed equivalent to the surface of the stainless steel baskets. Following Equation5.8, the emissivity of the stainless steel was calculated to be 0.36.

5.4.3 Varying Ambient Temperature

A few additional tests were run to examine the effect of a different temperature. For the stainless steel surface tests with the 7.5 *cm* cube, a test was run at 200 °C with the fan on and with the fan off. Further, a test was run on the 10 *cm* basket at 200 °C with the fan on to observe the effect of a different basket size. The results of the additional tests are graphed below.

	Max Fan Speed		Fan Off	
	100 °C	200 °C	100 °C	200 °C
Basket Width, $2r$ (cm)	h (W/m^2K)	h (W/m^2K)	h (W/m^2K)	h (W/m^2K)
7.5	28.3	31.0	5.6	7.2
10	23.4	30.8		

Table 5.2: Effect of higher temperature for heat transfer tests

5.5 Discussion of Heat Transfer Results

5.5.1 Comparison of Results between Heat Transfer Test and Previous Methods

O'Conner's method, which used smooth surfaced aluminum spheres in a convection oven, showed heat transfer coefficient results ranging between 19 and 22 W/m^2K for spheres of diameter 1.5 to 4 inches at 143.2 °C. The fan of the oven was on, though the speed was not recorded. It was assumed that the mixing action of his oven closely matched ours, and an air velocity of 1.6 *m/s*. With the sphere diameters of 2", 3", and 4" used by O'Conner, the specimens of similar sizes from the proposed heat transfer test best compared to the cubes of width 5.0, 7.5, and 10.0 cm.

Cube Width (cm)	Calculated *h* from Sphere in Stirred Bath at 143.2 °C (W/m^2K)	O'Conner's AL Sphere Results at 143.2 °C (W/m^2K)	Calculated *h* from Sphere in Stirred Bath at 100 °C (W/m^2K)	AL Covered Cube Heat Transfer Experiment at 100 °C (W/m^2K)
5	19.3	21.2	20.3	16.5
7.5	15.6	20.1	16.4	8.9
10	13.4	20.0	14.1	6.4

Table 5.3: Comparing experimental, calculated, and O'Conner's results for aluminum

As seen in the table above, the results found using the aluminum covered mesh cubes were lower than O'Conner's results. This was expected since the lower oven temperature yielded lower heat transfer coefficients. Further, the cube tests had aluminum foil lining the surface of the oven, where O'Conner's experiments kept the stainless steel oven surface exposed. The aluminum foil oven lining in the presented method reduced the radiation emitted to the baskets since the emissivity of the oven was lower, ultimately lowering the heat transfer coefficients. Additionally, the aluminum foil lining in the oven may have resulted in lower air mixing since it may have slowed the air

velocities. Since the correlation did not apply to the cube shape, the intention of the comparison between the calculated and experimental values was to show that the experiment gave reasonable results.

Examining the fluctuation of heat transfer with varying specimen sizes, it is unknown why O'Conner's data stayed relatively constant for the 3 sizes examined. His result for the 5 *cm* specimen was exceptionally close to the calculated data from the Nusselt correlation, however, does not show similar reduction in heat transfer with increasing sample sizes. Therefore, it is recommended that the heat transfer coefficient be found for each basket size used in the Frank-Kamenetskii method.

Two to three additional trials were run for the stainless steel basket sizes with maximum fan speed to show variance between runs. The standard deviation constantly decreased as the size of the basket increased. This was most likely due to the better insulation ability of the larger baskets. The precision of determining *h* seems to increase with the larger baskets. In addition, running tests in larger baskets will yield better extrapolation to large-scale applications. For these reasons, if it recommended to runs standard oven tests and heat transfer tests for larger baskets to increase accuracy. The larger baskets require more preparation and material, so choose basket sizes up to ones that fit into the financial budget.

There was an unexpected increase in *h* from the 10 *cm* basket to the 15 *cm* for both the stainless steel and aluminum foil baskets with the maximum fan speed. However, the increase was not seen for either basket with the oven fan off. This increase may have been due to a difference in air circulation patterns within the convection oven. Since the baskets were different sizes, the surfaces were in different locations within the

oven. Any inconsistencies in the mixing action could have impacted the heat transfer to the baskets.

5.5.2 Comparison to Nusselt Correlations

Examining the heat transfer coefficient results with the heat transfer values obtained from the Nusselt correlation for a vertical plate in Equation 5.14, the results can be seen below in Table 5.4.

Cube Width (cm)	Calculated *h* for Free Convection to Vertical Plate (Equation 5.14) (W/m^2K)	*h* Experimental from Free Convection on AL Covered Cube (W/m^2K)
2.5	10.7	5.2
5.0	9.0	3.7
7.5	8.1	2.9
10.0	7.6	2.3
15.0	6.8	2.1

Table 5.4: Comparison of experimental results AL lined basket with *Nu* correlation

The experimental results for the low radiation free convection runs are lower than the calculated values from the Nusselt correlation. The Nusselt calculations are for an ideal isothermal plate, however, the experimental values were probably lower due to the small heat loss into insulated basket. Further, since there was not a Nusselt correlation for the cube shape, a vertical plate correlation was used since the cube side was like a vertical flat plate. Since the shape for the calculation and experiment differ, the closeness in *h* values were reasonable. The calculated values showed that the experimental results were on the same order and the numbers seemed reasonable for the wire-mesh baskets.

5.5.3 Estimation of the Radiative Heat Transfer Coefficient

The calculated emissivity of 0.36 for the rough stainless steel basket was found to be higher than the value listed by Incropera for clean stainless steel, however, the calculated value closely matched listed values for lightly oxidized stainless steel at 0.33. The lightly oxidized value was a better estimate since previous oven basket tests generated smoke that lightly stained the oven despite cleaning efforts on the oven surface.

5.5.4 Varying Ambient Temperature

As expected, the higher oven temperature resulted in a higher heat transfer coefficient for both the case of maximum fan speed and no fan. With regards to the 10 *cm* basket, the increase in temperature with the fan on showed increase in h. In contrast, the 7.5 *cm* basket exhibited smaller increase in h. The calculated increase in radiation due to the temperature increase was 1.7 W/m^2K. From the 7.5 *cm* basket, radiation may have the largest affect on h for oven temperatures within this range. Further heat transfer tests over a range of temperatures would need to be run to show the true affect of radiation and convection with varying temperatures.

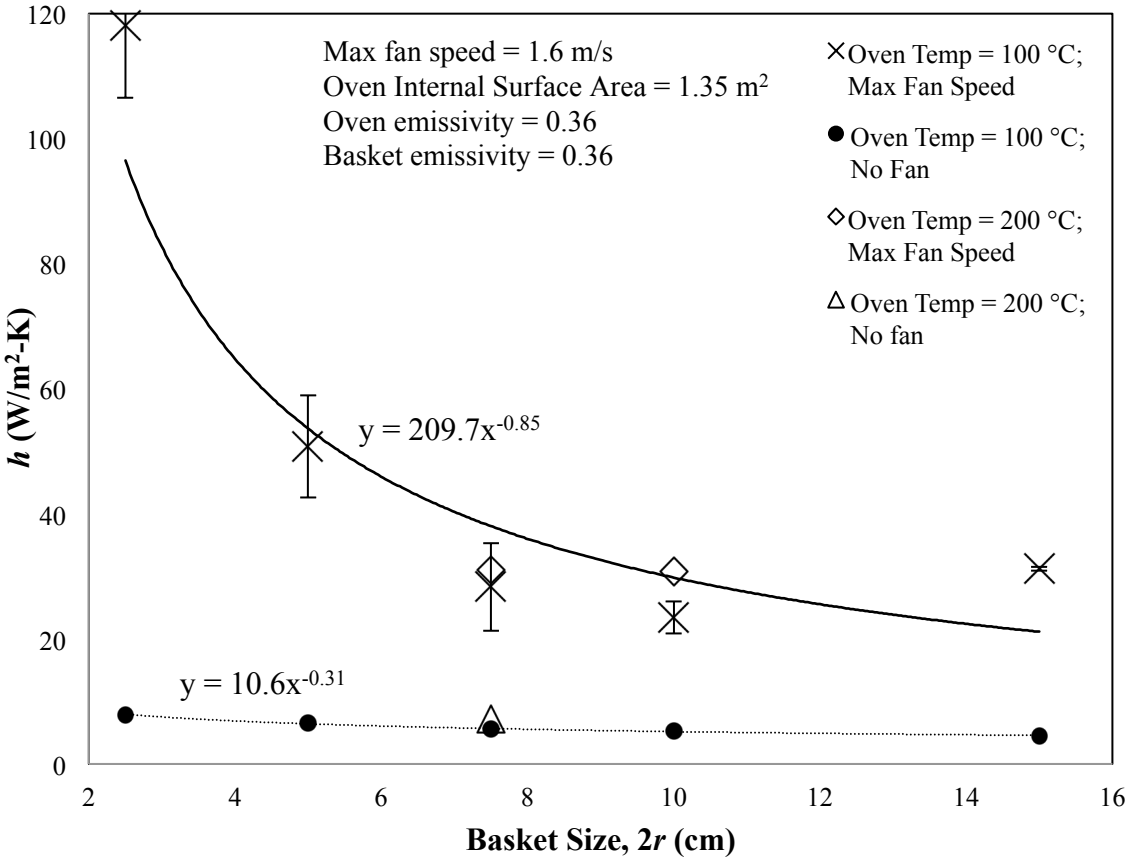

Figure 5.5: Increasing the oven temperature from 100 °C to 200 °C showed very small change in h

Though there was increase in h with higher temperature, the increase was very small, as seen Figure 5.5. For this reason, h data from the 100 °C experiments could directly be used to determine h values for experiments at 200 °C. Therefore, if a convection oven has similar characteristics (emissivity, fan speed, dimensions) to the oven used in the experiment, the equation from the 100 °C runs may be used if desired temperature approximately is near the range 100-200 °C. From the power function for the 100 °C stainless steel basket curve with maximum fan speed, an estimation of the heat transfer coefficient for basket sizes $2.5cm \le 2r \le 15cm$ may be found using:

$$h_{tot} \approx 209.7(2r)^{-0.85} \tag{5.16}$$

For $T_A \approx 100-200\,^{\circ}C$, $u_\infty \approx 1.6\,m/s$, $\epsilon_S \approx \epsilon_O \approx 0.36$ where r is in cm. Similarly, the equation from the power function of the free convection (no fan) experiments may be used to estimate the heat transfer coefficient for ovens of similar characteristics.

$$h_{tot} = 10.6(2r)^{-0.31} \tag{5.17}$$

For $T_A \approx 100-200\,^{\circ}C$, $u_\infty \approx 0.0\,m/s$, $\epsilon_S \approx \epsilon_O \approx 0.36$ where r is in cm.

5.6 Conclusion

The method for calculating the heat transfer in a convection oven can be useful for fire investigators applying the Frank-Kamenetskii model to examine spontaneous ignition. Having accurate heat transfer data will yield a better finite Biot correction factor and ultimately more precise P and M properties. Theory for the method allowed the equation

$$\boxed{h_{tot} \approx \left[\frac{(mc)_{AL} + (mc)_{SS}}{S}\right]\frac{\left(\frac{dT_s}{dt}\right)_i}{(T_\infty - T_i)}}$$

to be used to calculate the heat transfer coefficient between the oven and basket surface. The method presented gave reasonable results and was implemented with the same stainless steel baskets used with determining critical temperatures for a sample. It was easy to apply and required little additional supplies. If a convection oven with approximately similar characteristics (fan speed, emissivity, dimensions) is used, Equations 5.16 and 5.17 may be used to estimate heat transfer coefficients between the basket surface and oven air for a temperature range approximately between 100 °C and 200°C.

Chapter 6: Conclusion

A method of determining the likeliness of spontaneous ignition has been provided through the Frank-Kamenetskii method. This method can be a helpful tool for fire investigators examining reactive porous solids under the case of the following scenarios: a cold material in a hot environment, a material layer on a hot surface, and a hot material in a cold environment. To simplify the chemical analysis process in determining criticality, a method of determining material constants, P and M, has been described using a standard oven test to find critical ambient temperatures. Additionally, a list of known P and M values has been collaborated to provide reference in examining common self-heating materials.

Many factors are ignored in the basic self-heating theory, including diffusion of oxygen, moisture, non-conduction heating within the substance, mixtures with competing reactions, and transient effects. For this reason, the presented method should be used merely as a guide for determining the likelihood of spontaneous ignition. The ignored factors may have affects on the accuracy of the model, so it is important to increase accuracy in areas that may be corrected. These correctable factors are for the case of a finite Biot number, low activation energy, and reactant consumption. The reactant consumption has shown to be difficult to implement due to the required parameters within the chemical process. Still, a rough estimate of the reaction order, and a and b values will be feasible in implementing the consumption factor. An example used by Bowes (Bowes, 1984) was given to help describe the procedure of applying all of the available corrections.

For correcting the self-heating case with a finite Biot number at the surface of the material, a method has been derived from the energy balance of a test basket in a convection oven. The method is simple to implement and is mainly used with existing materials from a standard oven test. The additional supplies required are aluminum foil and kaowool, and bare little added financial expense. Tests were run in a convection oven, to ensure the validity of the derived heat transfer method. The results for the heat transfer coefficients were compared to known Nusselt correlations and the comparison seemed reasonable. The method is recommended for correcting critical Damkohler numbers for the standard oven tests. The heat transfer test should be run for the temperatures in range of the critical ambient temperatures of the samples used. The heat transfer results varied with basket sizes due to the differing lengths and air circulation patterns. Therefore, the heat transfer test should be performed for each basket size used in testing.

As described, scaling to large-scale fires may result in errors. The largest range of baskets that are financially applicable should be used to reduce this error. The larger baskets were also shown to increase the precision of the heat transfer tests, which may additionally increase the accuracy of the heat transfer corrections.

The proposed heat transfer test was also used to calculate the radiation emitted from the convection oven by analyzing samples low and high radiation. The resulting emissivity of the convection oven used in the described tests was determined to be 0.36. With the light soot residue on the oven walls and baskets, this value closely matched the listed value of lightly oxidized stainless steel.

Spontaneous ignition has caused extensive financial loss and many fatalities in historical fire events. In the investigations of these cases, the phenomena is difficult to investigate due to the destruction of evidence from the fire and improper analysis of self-heating. The intent of this thesis is to assist fire investigators with the concept of spontaneous ignition, and to provide testing and analysis methods to assist in diagnosis.

Appendices

A. Select Temperature vs. Time Graphs from Heat Transfer Experiments

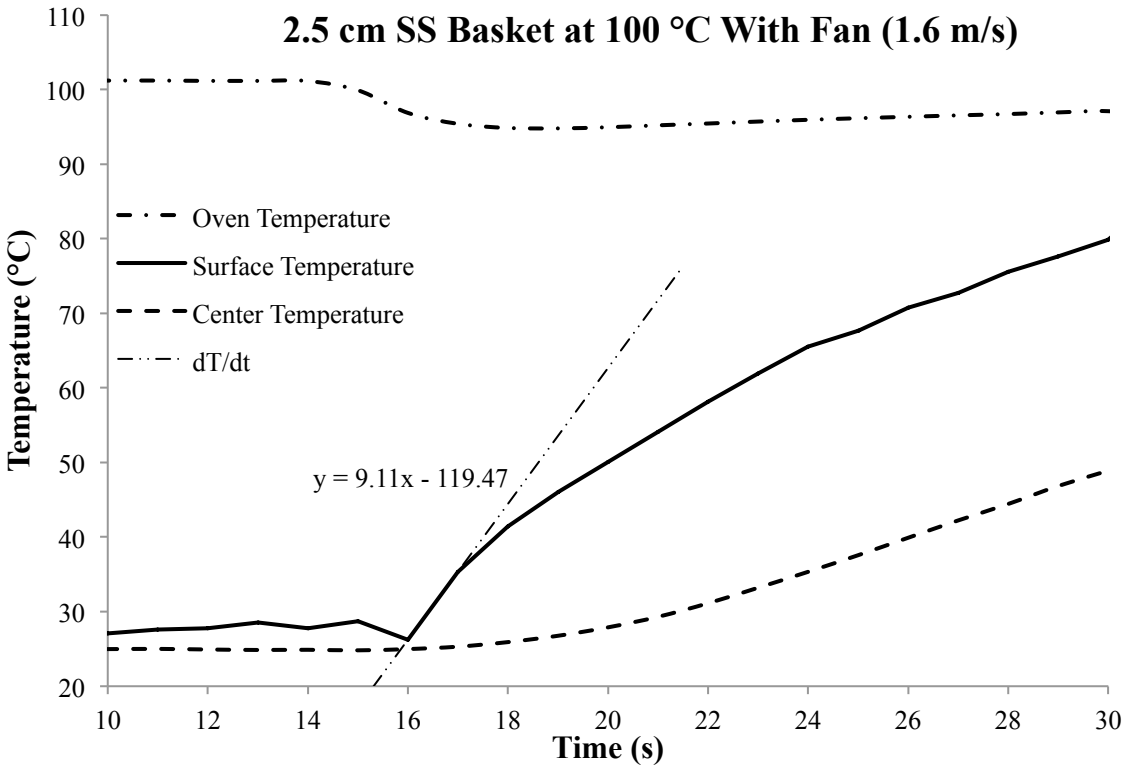

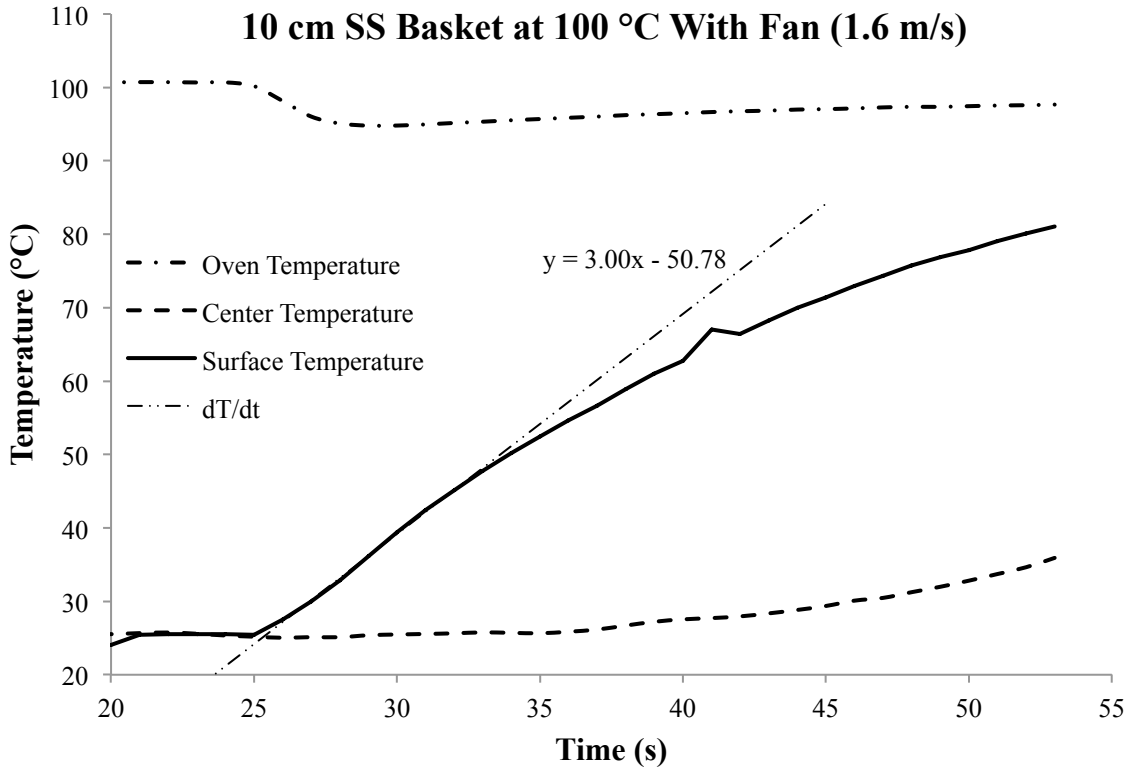
10 cm SS Basket at 100 °C With Fan (1.6 m/s)
Temperature (°C)
Time (s)
Oven Temperature
Center Temperature
Surface Temperature
dT/dt
y = 3.00x - 50.78
110
100
90
80
70
60
50
40
30
20
20
25
30
35
40
45
50
55

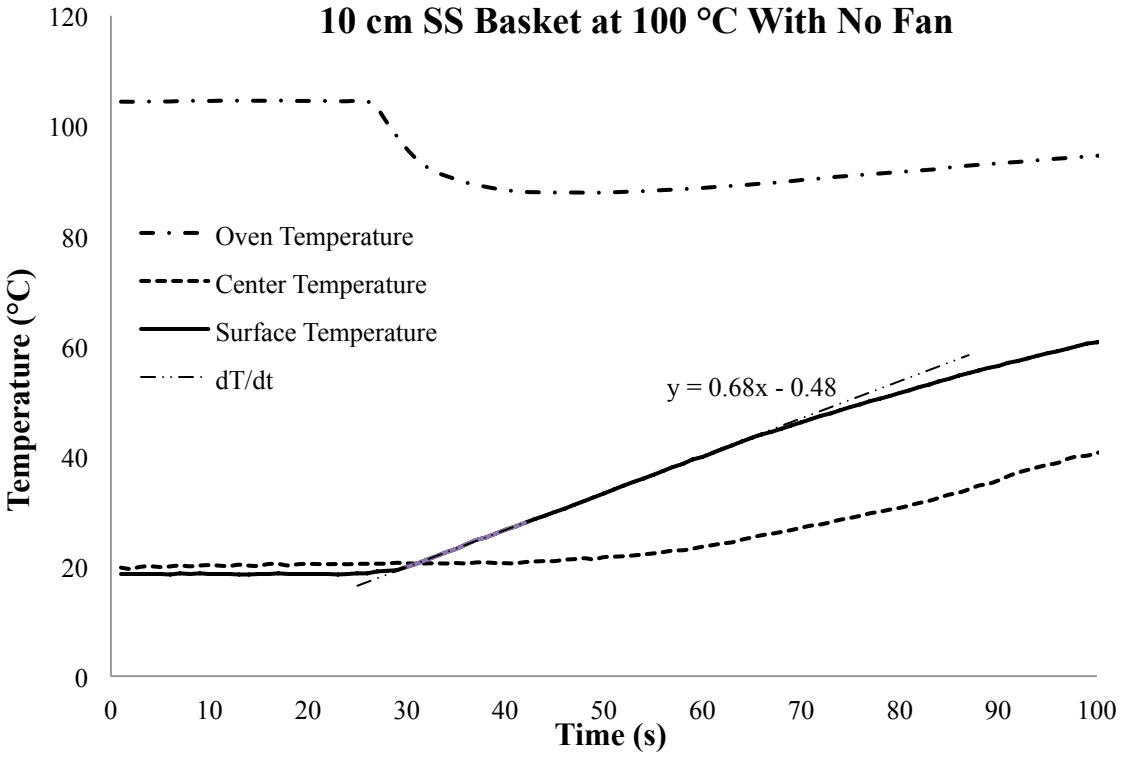
10 cm SS Basket at 100 °C With No Fan
Temperature (°C)
Time (s)
Oven Temperature
Center Temperature
Surface Temperature
dT/dt
y = 0.68x - 0.48
120
100
80
60
40
20
0
0
10
20
30
40
50
60
70
80
90
100

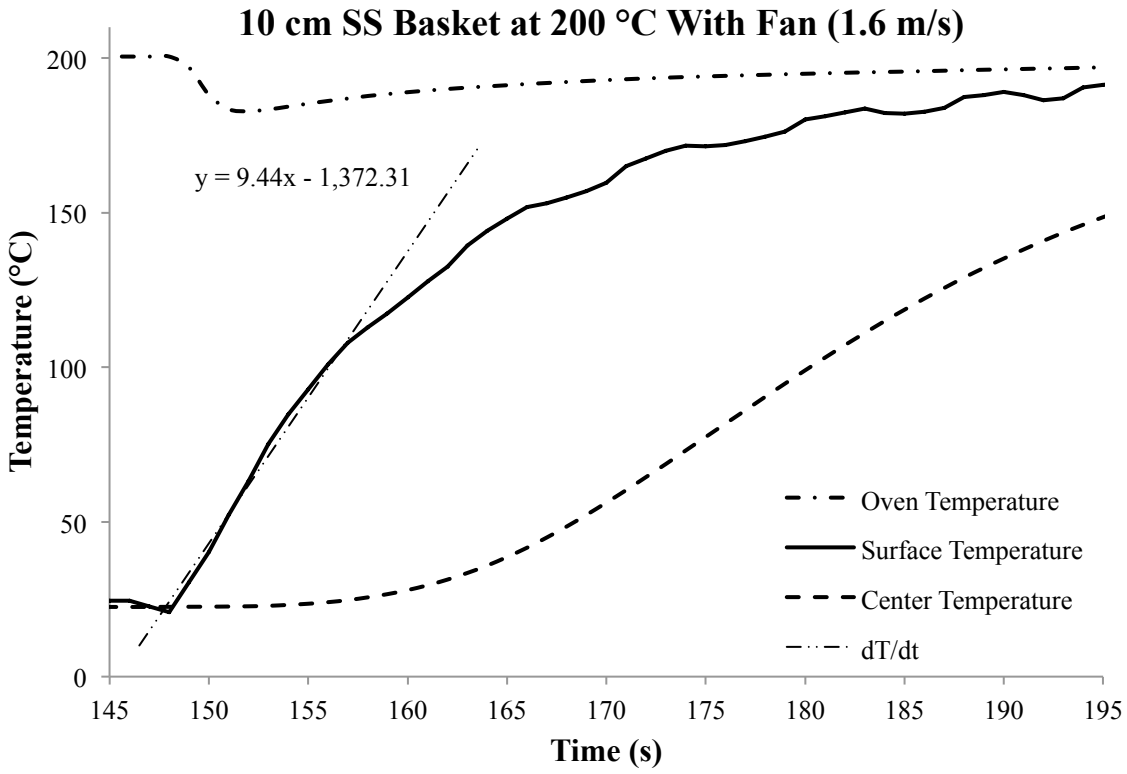
10 cm SS Basket at 200 °C With Fan (1.6 m/s)
Temperature (°C)
Time (s)
y = 9.44x - 1,372.31
Oven Temperature
Surface Temperature
Center Temperature
dT/dt
0
50
100
150
200
145
150
155
160
165
170
175
180
185
190
195

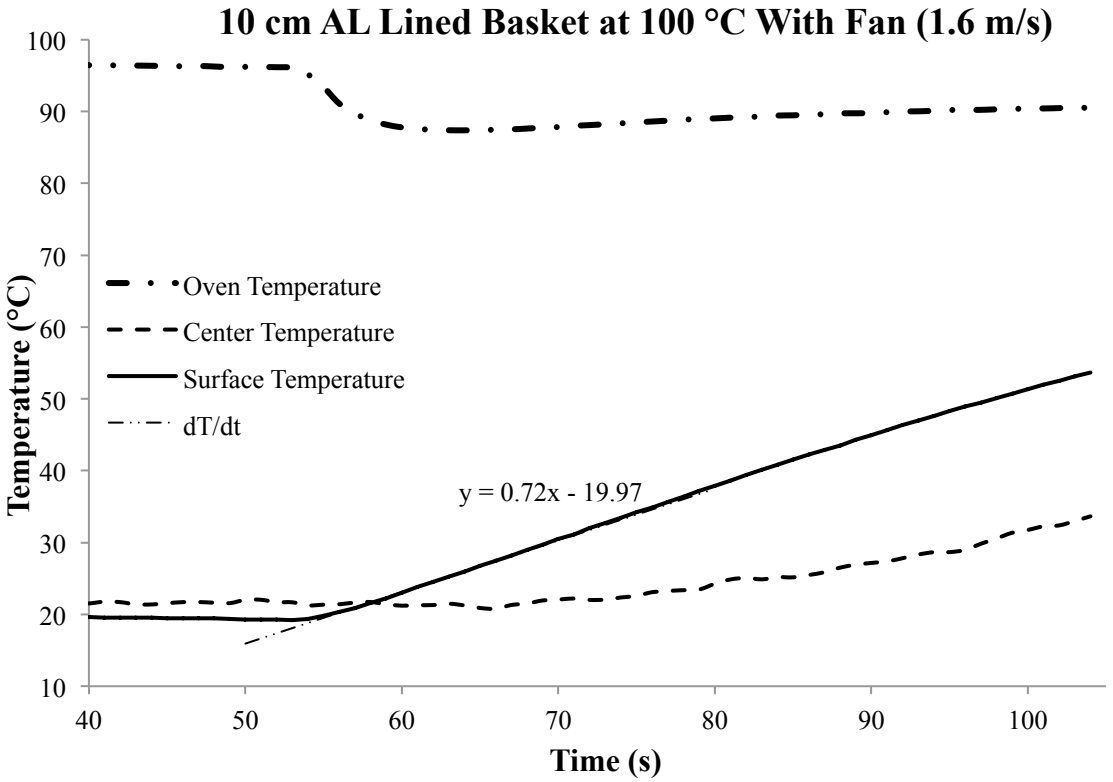
10 cm AL Lined Basket at 100 °C With Fan (1.6 m/s)
Temperature (°C)
Time (s)
y = 0.72x - 19.97
Oven Temperature
Center Temperature
Surface Temperature
dT/dt
10
20
30
40
50
60
70
80
90
100
40
50
60
70
80
90
100

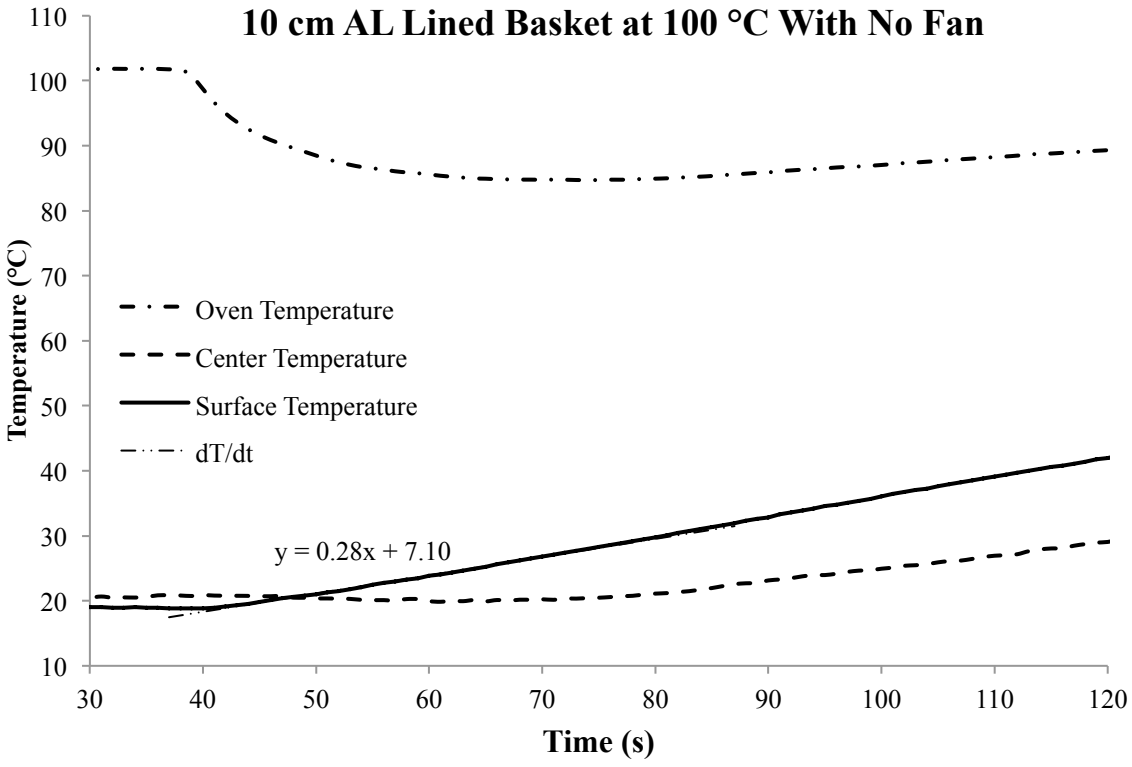
10 cm AL Lined Basket at 100 °C With No Fan
Temperature (°C)
Time (s)
Oven Temperature
Center Temperature
Surface Temperature
dT/dt
y = 0.28x + 7.10
110
100
90
80
70
60
50
40
30
20
10
30
40
50
60
70
80
90
100
110
120

B. P and M Database Sorted According to Hazard

A hypothetical scenario was established to examine the hazard of each material listed in the *P* and *M* database (Section 4.5). The scenario was considered for a cube under ideal conditions ($\delta_c = 2.52$) where T_A = 32 °C (90 °F) and the width (2*r*) of the cube is 2*m*. The Damkohler number for each specific material cube was found from Equation 4.3 for the listed *P* and *M* values, and given conditions. The explosives listed in Section 4.5 were determined not to be a spontaneous ignition hazard under the given conditions, so they were not listed here. The classification of the hazard was based on the *P* and *M* values listed in the literature.

Highest Risk (Very Likely)

Material	P (*K*)	M*	E (*kJ/mol*)	Comments	Source	$\frac{\delta}{\delta_c}$
Milk Powder	9502	34.7	79	skim milk from temperature range 142 – 171 °C	(Beever P. , 1984)	150.1
Calcium Hypochlorite	5833	19.5	48.5	hydrated. Values are for low temperature regime	(Gray & Halliburton, 2000)	6.3
Mineral Wool	6800	21.6	56.54		(Spokoinyi & Eidukyavicius, 1988)	2.2
Distiller's Dark Grains	8046	25.3	66.9		(Bowes, 1984)	1.5

High Risk (Likely)

Material	P (*K*)	M*	E (*kJ/mol*)	Comments	Source	$\frac{\delta}{\delta_c}$
Spent Brewing Grains	6495	19.9	54		(Walker, 1961)	1.07
Animal Feedstuff	8404	26.06	70		(Bowes, 1984)	0.97

Medium Risk (Not Likely)

Material	P (K)	M*	E (kJ/mol)	Comments	Source	$\frac{\delta}{\delta_c}$
Plywood (Plain)	10572	32.9	87.9	calculated directly from E,Q,A, density, and conductivity for plain plywood	(Loftus, 1985)	0.74
Plywood (Fire Rated)	11570	35.7	96.2	calculated directly from E,Q,A, density, and conductivity for fire rated plywood	(Loftus, 1985)	0.46
Milk Powder	9538	28.7	79.3	skim milk from temperature range 138 – 173 °C and density 600 kg/m^3	(O'Connor, 1990)	0.33
Coal	8419	25	70	bituminous South African with volatile content of 26% over 120-220 °C temperature range	(Tognotti, Petarca, & Zanelli, 1988)	0.32
Milk Powder	9754	29.4	81.1	milk with 30% fat added from temperature range 130 – 200°C	(J.G. & Synnott, 1988)	0.33

Low Risk (Highly Unlikely for the given conditions)

Material	P (K)	M*	E (kJ/mol)	Comments	Source	$\frac{\delta}{\delta_c}$
Eucalyptus Leaves	8539	24.5	71	leaves were at density 140 kg/m^3	(Jones & Raj, 1988)	0.13
Calcium Hypochlorite	14793	44.5	123	hydrated. Values are for high temperature regime	(Gray & Halliburton, 2000)	0.08
Carbon (Activated)	10007	28.2	83.2	oven-cube tests on powdered activated charcoal over 50-190 °C temperature range	(Nelson, 1992)	0.04
Charcoal (Activated)	12700	36.975	106	weathered	(Cameron & MacDowall, 1972)	0.04
Milk Powder	11979	34.2	99.6	milk with 44% fat added from temperature range 135 – 175°C	(Duane & Synnott, 1992)	0.03
Forest Floor Material 1	9862	27.2	82		(Jones et al, 1990)	0.03
Forest Floor Material 2	10945	30.2	91		(Jones et al, 1990)	0.01
Charcoal (Activated)	11666	28.1 - 35.7	97	all types except the 3 minimally hazardous products from oven-cube tests of 10 types	(Cameron & MacDowall, 1972)	0.01
Wheat Flour	15539	44.2	129.2		(Nelson, 1992)	0.01

Low Risk (Highly Unlikely for the given conditions)

Material	P (K)	M*	E (kJ/mol)	Comments	Source	$\frac{\delta}{\delta_c}$
Cork (Solid)	9622	23.9	80	calculated directly from E,Q,A, density, and conductivity from values based on small-specimen tests in adiabatic furnace	(Gross & Robertson, 1958)	0.00
Cork (Dust)	13711	37.2	114	oven basket method	(Hensel, 1988)	0.00
Cotton	11282	28.6	93.8	based on oven-basket method on cotton fibers of	(Gray, Little, & Wake, 1992)	0.00
Rice Husks	12629	32.5	105	small scale oven-cube test with density 140 kg/m^3	(Jones & Raj, 1988)	0.00
Fertilizer (12-13-6)	17319	47.9	144	based on oven-basket data for 12-13-6 fertilizer	(Huygen & Perbal, 1965)	0.00
Milk Powder	9056	20.5	75.3	whole milk from temperature range 145 – 165 °C	(Chong, Chen, & Mackerth, 1999)	0.00
Bagasse	13000	33.08	108		(Bowes, 1984)	0.00
Yeast Powder	16640	44.5	138		(Bowes, 1984)	0.00
Cellulose Insulation	13230	32.8	110	unretarded cellulose from adiabatic furnace test	(Issen, 1980)	0.00
Ammonium Nitrate	16237	42.2	135	fertilizer grade with 7% additional fuel added	(Hainer, 1954)	0.00
Milk Powder	11678	26.2	97.1	skim milk from temperature range 135 – 170 °C and	(Chong, Chen, & Mackerth, 1999)	0.00
Cotton	17319	41.4	144	calculated directly from E,Q,A, , and conductivity from values based on small-specimen tests in adiabatic furnace	(Gross & Robertson, 1958)	0.00
Ammonium Nitrate	17921	43.2	149	fertilizer grade	(Hainer, 1954)	0.00
Milk Powder	19292	45.5	160.4	(E seems high) whole milk from temperature range 130 – 145 °C	(Chong, Chen, & Mackerth, 1999)	0.00
Cellulose Insulation	13591	26.5	113	hot-plate method with density of 34 kg/m^3	(Ohlemiller & Rogers, 1980)	0.00
Cellulose Insulation	15876	30.1	132	insulation retarded with 20% boric acid using hot-plate method with density of 41 kg/m^3	(Ohlemiller & Rogers, 1980)	0.00

Bibliography

ASTM Standard E659-78. (2005). "Standard Test Method for Autoignition Temperature of Liquid Chemicals". West Conshohocken, Pennsylvania: ASTM International.

Babrauskas, V. (2003). *Ignition Handbook.* Issaquah, Washington: Fire Science Publishers.

Barzykin, V., Gontkovskaya, V., & Merzhanov, A. (1966). Theory of Thermal Explosion of Self-Accelerating Reactions. *Combustion, Explosion, and Shock Waves , 2* (4), 11-13.

Beever, P. F. (1988). Self-Heating and Spontaneous Combustion. In P. J. DiNenno, *SFPE Handbook* (1st Edition ed., pp. 1:341-1:351). NFPA.

Beever, P. (1984). Spontaneous Ignition of Milk Powders in a Spray-Drying Plant. *Journal of Dairy Technology , 37*, 68-71.

Bowes, P. C. (1984). *Self-Heating: Evaluating and Controlling the Hazards.* New York, New York: Elsevier.

Cameron, A., & MacDowall, J. (1972). The Self-Heating of Commercial Powdered Activated Carbons. *Journal of Applied Chemistry and Biotechnology , 22*, 1007-1018.

Carson, J. K., Willix, J., & North, M. F. (2006). Measurements of Heat Transfer Coefficients within Convection Ovens. *Journal of Food Engineering , 72*, 293-301.

Chong, L., Chen, X., & Mackerth, A. (1999). Effect of Ageing and Composition on the Ignition Tendency of Dairy Powders. *Journal of Food Engineering , 39*, 269-276.

Contship Containerline Ltd. v. PPG Industries Inc., 05-0267-cv (United States Court of Appeals for the Second Circuit March 21, 2006).

Darling, J. A. (1999, September). Calcium Hypochlorite: Fire In The Hold. *IUMI Conference* , 1-10.

DG Harmony v. PPG Industries Inc., 05-6116-cv (United States Court of Appeals for the Second Circuit July 9, 2008).

Dobratz, B., & Crawford, P. (1985). *LLNL Explosives Handbook: Properties of Chemical Explosives and Explosive Simulants.* Livermore, CA: Lawrence Livermore National Laboratory.

Duane, T., & Synnott, E. (1992). Ignition Characteristics of Spray-Dried Milk Product Powders in Oven Tests. *Journal of Food Engineering , 17*, 163-176.

Frank-Kamenetskii. (1939). Temperature Distribution in Reaction Vessel and Stationary Theory of Thermal Explosion. *Journal of Physical Chemistryl , 13*, 738-755.

Gray, B. (2002). Spontaneous Combustion and Self-Heating. In P. J. DiNenno, *SFPE Handbook of Fire Protection Engineering* (3rd Edition ed., pp. 2-211:2-228). Quincy, Massachusetts: Courier/Westford.

Gray, B., & Halliburton, B. (2000). The Thermal Decomposition of High Grade Bleaching Powder. *Journal of Chemical Technology and Biotechnology , 35*, 223-239.

Gray, B., Little, S., & Wake, G. (1992). The Prediction of a Practical Lower Bound for Ignition Delay Times and a Method of Scaling Times-to-Ignition in Large Reactant Masses from Laboratory Data. *24th Symposium (International) on Combustion* , 1785-1791.

Gross, D., & Robertson, A. (1958). Self-Ignition Temperatures of Materials from Kinetic-Reaction Data. *Journal of Research and National Institute of Standards , 61*, 413-417.

Hainer, R. (1954). The Application of Kinetics to the Hazardous Behavior of Ammonium Nitrate. *5th Symposium on Combustion* , 224-230.

Hensel, W. (1988). Entzundung abgelagerter Staube. *VDI Berichte Nr. , 701*, 143-166.

Huygen, D., & Perbal, G. (1965). The Decomposition of Compound Fertilizers. *1965 Technical Conference* (p. LEE/65/XIII). Paris: International Fertilizer Industry.

Incropera. *Fundamentals of Heat Transfer.*

Issen, L. (1980). *Fire Performance of Loose Fill Cellulosic Insolation in Residential Occupancies - A Progress Report (NBSIR 80-2085).* NBS.

J.G., O., & Synnott, E. (1988). Influence of Sample Shape and Size on Self-Ignition of a Fat-Filled Milk Powder. *Journal of Food Engineering , 7*, 271-280.

Jones, J., & al, e. (1990). The Self-Heating and Thermal Ignition Propensity of Forest Floor Litter. *Journal of Fire Sciences , 8*, 207-223.

Jones, J., & Raj, S. (1988). The Self-Heating and Ignition of Vegetation Debris. *Fuels , 67*, 1208-1210.

Jones, J., & Wade, M. (1999). Direct Determination of the Biot Number in Oven Heating Tests. *Journal of Fire Sciences , 17*, 421-429.

Kreith, F., & Bohn, M. S. (2001). *Principles of Heat Transfer* (6th Edition ed.). Pacific Grove, California: BROOKS/COLE.

Loftus, J. (1985). *Self-Heating to Ignition Measurements and Computation of Critical Sizes for Solar Energy Collector Materials (NBSIR 85-3122).* NBS.

Maiden, D. (1987). *A Model for Calculating the Threshold for Shock Initiation of Pyrotechnics and Explosives.* Livermore, CA: Lawrence Livermore National Lab.

Mitchell, N. D. (1951, October). New Light on Self-Ignition. *NFPA Quarterly* , 165-172.

Nelson, M. (1992). Detection and Extinction of Fire and Smouldering in Bulk Powder. *British Materials Handling Board* , 64-139.

O'Connor, J. F. (1990). *Self-heating and Self-ignition in Dairy Powders.* Michigan State University, Department of Agricultural Engineering. Dissertation.

Ohlemiller, T., & Rogers, F. (1980). Cellulosic Insulation Material. II. Effect of Additives on Some Smolder Characteristics. *Combustion Science and Technology , 24*, 139-152.

Routley, J., Jennings, C., & Chubb, M. (1991). *High-rise Office Building Fire: One Meridian Plaza Philadelphia, Pennsylvania.* Federal Emergency Management Agency, United States Fire Administration National Fire Data Center, Emmitsburg.

Sakin, M., Kaymak-Ertekin, F., & Ilicali, C. (2009). Convection and Radiation Combined Surface Heat Transfer Coefficient in Baking Ovens. *Journal of Food Engineering , 94*, 344-349.

Skinner, D., Olson, D., & Block-Bolten, A. (1998). Electrostatic Discharge Ignition of Energetic Materials. *Propellants, Explosives, Pyrotechnics , 23*, 34-42.

Spokoinyi, F., & Eidukyavicius, K. (1988). Mechanism of Spontaneous Ignition during Storage of Mineral Wool Objects. *Combustion, Explosion and Shock Waves , 24*, 649-651.

The Gillette News. (2004, June 01). *Fire at Buckskin Mine Causes $200,000 Damage*. Retrieved February 16, 2011, from gillettenewsrecord.com: http://www.gillettenewsrecord.com/articles/2004/06/01/news/news4.txt

Thomas, P. (1958). On The Thermal Conduction Equation for Self-Heating Materials with Surface Cooling. *Transactions of the Faraday Society , 54*, 60-65.

Tognotti, L., Petarca, L., & Zanelli, S. (1988). Spontaneous Combustion in Beds of Coal Particles. *22nd Symposium (International) on Combustion* , 201-210.

Walker, I. (1961). Spontaneous Ignition of Spent Brewing Grains. *New Zealand Journal of Science , 4*, 1961.

Weather Underground. (n.d.). *History for Albany, NY: Saturday, June 17, 1950*. Retrieved July 14, 2010, from www.wunderground.com